Pergamon

0042-6989(94)E0034-I

Vision Res. Vol. 34, No. 18, pp. 2337–2355, 1994

0042-6989/94 $7.00 + 0.00

Extensive Integration Field Beyond the Classical Receptive Field of Cat's Striate Cortical Neurons—Classification and Tuning Properties

CHAO-YI LI,*† WU LI*

Received 18 January 1993; in revised form 14 October 1993

Length- and width-summation curves of striate cortex cells revealed that there exist facilitatory, inhibitory or disinhibitory integration fields (IF) beyond the sides and ends of the classical receptive field (RF). The extent of the IFs is most frequently 2–5 times the size of the RFs. The tuning properties of IFs were studied using an annular surround grating patch while an optimal centre patch was placed at the excitatory RF to continuously activate the cell. The results show that, for most cells, the orientation, spatial frequency and speed tuning of the IFs were similar to, but broader than, the tuning of the RF, whereas the direction selectivity of the IF was not as pronounced as that of the RF. The possible functional significance of the IF is discussed.

Cat Visual cortex Receptive field Spatial integration Tuning properties Periphery effects

INTRODUCTION

In the retina and lateral geniculate nucleus, it is well known that stimuli presented far beyond the receptive field (RF) may strongly influence neuronal responses to stimuli presented within the RF centre (McIlwain, 1964, 1966; Cleland, Dubin & Levick, 1971; Ikeda & Wright, 1972a, b; Krüger & Fischer, 1973; Fischer & Krüger, 1974; Krüger, 1977; Marrocco, McClurkin & Young, 1982). These periphery effects were found mainly in the transient or Y-cells (Cleland *et al.*, 1971; Ikeda & Wright, 1972c; Krüger, 1977). By analysing the spatial summation properties of retinal ganglion cells and lateral geniculate neurons in cat with flashing bars of different lengths or spots of different sizes, we have demonstrated an extensive disinhibitory region (DIR) in both X- and Y-cells outside the inhibitory surround of their RFs (Li & He, 1987; Li, Pei, Zhow & Mitzlaff, 1991; Li, Zhou, Pei, Qiu, Tang & Xu, 1992). The extent of the DIR may reach 15 deg or more.

Similar experiments have also been conducted in striate cortex. By measuring the effect of moving a second stimulus outside the RF on the responses to stimuli located inside the RF, or by measuring responses to gratings of an increasingly large number of cycles centred on the cells' RFs, either facilitatory or inhibitory surround effects can be observed (Hubel & Wiesel, 1965; Jones, 1970; Blakemore & Tobin, 1972; Bishop, Coombs & Henry, 1973; Creutzfeldt, Kuhnt & Benevento, 1974; Hess, Nigishi & Creutzfeldt, 1975; Maffei & Fiorentini, 1976; Fries, Albus & Creutzfeldt, 1977; Nelson & Frost, 1978; Rizzolatti & Camarda, 1977; De Valois, Thorell & Albrecht, 1985). However, the strength and extent of the surround effect reported varied considerably between the different studies.

The present experiments were undertaken to delimit the remote surround area of striate cortex neurons and to examine strength of facilitatory and/or inhibitory influences originating from this area. As this extensive region was revealed by spatial integration and no response could be elicited when it was stimulated in isolation, we refer to it as the *integration field* (IF) in this report. In order to study the remote integration field, the classic RF must be delimited. We tried three methods, based on stationary flashing light profiles, profiles obtained with small grating patches and a masking method as described below. These methods are compared quantitatively. In general, we preferred the masking method to detect the weak border of the excitatory RF. The mask was always circular. The primary aim of this study was to test the tuning properties of the IF in the domains of orientation, direction, spatial frequency and movement speed using sine-wave gratings, and to compare them with the tuning properties of the receptive field *per se* for these cells.

*Department of Sensory Information Processing, Shanghai Institute of Physiology, Chinese Academy of Sciences, 320 Yue-Yang Road, Shanghai 200031, People's Republic of China [*Fax* 86-21-433 2445].
†To whom all correspondence should be addressed.

METHODS

Preparation

Experiments were performed on adult cats weighing between 2.5 and 3.5 kg. The preparation and recording techniques were identical to those described in detail in previous papers (Li & He, 1987; Li *et al.*, 1991, 1992) and are described briefly here. The animals were anaesthetized prior to surgery with an i.m. injection of Ketanest (30 mg/kg) and then tracheal and venous cannulation and bilateral cervical sympathectomy were carried out. The animal's head was fixed in a stereotaxic frame; a small opening of the skull was made over area 17 corresponding to the area centralis.

After the operation, the animals were immobilized using Flaxedil (20 mg/kg) and artificially respired. An i.v. infusion consisting of Flaxedil (10 mg/kg/hr), *d*-tubocurarine chloride (0.25 mg/kg/hr), urethan (20 mg/kg/hr) and glucose (200 mg/kg/hr) in Ringer's solution (1.5 ml/kg/hr) was maintained throughout the experiment. All wound margins and pressure points were treated with 1% Lidocaine. The end-tidal CO_2 was kept between 4–4.5% and rectal temperature was maintained at 37.8–38°C. ECG and heart rate were monitored. The nictitating membranes were retracted and pupils dilated. Special care was taken to maintain good optics: contact lenses were applied and supplementary lenses were used to focus the eyes on the screen at a distance of 30 cm in front of the eyes. The optic disks were plotted using the method of Fernald and Chase (1971), and the area centralis using the method of Bishop, Kozak, Levick and Vakkur (1962). Artificial pupils of 3 mm dia were used.

Recordings and stimulation

Single unit recordings were made by penetrating the dura mater over area 17 with a fine-tipped (1–1.5 μm dia, 5–10 μm long, 10–30 MΩ) tungsten-in-glass microelectrode. When a unit was isolated, the RF of the cell was aligned with centre of a monitor used to present the stimuli by adjusting the position of the latter. Cell discharges, after being standardized in amplitude, were fed into a personal computer (Hewlett-Packard Vectra 286/12) for subsequent data processing.

Visual stimuli were generated on the CRT screen (Textronix 608 monitor) of an image synthesizer (Picasso, Innisfree) under computer control. Light and dark bars and sine-wave gratings were presented at different orientations, spatial frequencies and velocities with real-time monitoring and analysis of the responses of the recorded cortical neurons. All measurements were made during stimulation of the dominant eye with the other eye occluded. The usual procedure was to present the stimulus over the receptive field centre, then the cells' tuning properties (orientation, direction, spatial frequency and speed) were determined by varying those parameters of the stimulus gratings in a random sequence. When a specific stimulus parameter was under investigation, all other parameters were kept at the optimal value for the cell.

RF profiles

Using optimally oriented stimuli, RF profiles were derived in two different ways: (a) a bar flashed alternately brighter then darker than a homogeneous background was moved across the RF in the width dimension [see inset in Fig. 1(A)], (b) a grating patch (on a homogeneous background) was moved across the RF. Within the patch the optimal grating drifted continuously in the neuron's preferred direction. The grating procedure allowed us to investigate RF profiles along the width and the length axes [see inset in Fig. 1(B) and (C) respectively]. The spatial summation properties of the cell were also determined with grating patches which were centred at the RF centre and set at the cell's optimal orientation, spatial frequency, direction and speed. For length-summation curves, patch width was held constant (equivalent to the RF's optimal width) and grating length varied between 0.1 and 18 deg in a random sequence [see inset in Fig. 4(A)]. Width summation properties were determined in a similar way, by varying the width of the patch with a constant length equivalent to the RF's optimal length [see inset in Fig. 3(A)]. Responses to each length (or width) were averaged for 10–20 cycles of the drifting grating, and standard errors were calculated for 5–20 repetitions.

Integration field

Having determined the dimensions and tuning properties of the RF, the tuning properties of the IF were then investigated. We used a circular grating patch at the RF centre to activate the cell continuously [resembling the activated discharge method of Henry, Bishop and Coombs (1969)], whose diameter was equal or slightly larger than the size of the receptive field of the cell under study. A concentric surround grating (outer diameter 18 deg, inner diameter equal to the diameter of the centre grating) was placed outside the excitatory RF. In the inset in Fig. 13(A) is shown the arrangement of the stimulus pattern. The surround gratings did not activate the cell when presented in isolation, but they often modulated the response of the cell to the grating patch within the receptive field. The strength of the surround effect (inhibition or facilitation) was dependent on the attributes (orientation, spatial frequency etc.) of the surround gratings. To minimize the effects of stray light, the mean luminance of the CRT screen was kept at 8.3 cd/m^2 and the contrast of the gratings $[(L_{max} - L_{min})/(L_{max} + L_{min})]$ between 0.2 and 0.5. The mean luminance of all gratings and "blanked" portions of the screen (e.g. Fig. 13 insets) was identical. Using this arrangement we could determine the tuning properties of the surround quantitatively in the domains of orientation, spatial frequency, speed and direction of movement.

To determine the configuration of the spatial summation (length and width) curves and the tuning functions of the RFs and their surround, 20–30 data points were usually collected within the testing range in a random fashion. The data were smoothed by a polynomial regression (of an order depending on the shape of the curve). Cells were classified into simple or complex

families according to (a) the separation or overlapping of the ON and OFF regions in response to a stationary, flashed bar (Hubel & Wiesel, 1962) and (b) the relative modulation of response (the ratio of the amplitude of the first harmonic to the mean response level, after subtraction of the average maintained rate) to drifting sinusoidal gratings (Skottun, De Valois, Grosof, Movshon, Albrecht & Bonds, 1991). Cells with separate ON and OFF regions [Fig. 1(A)] and relative modulation values above 1.0 were classified as simple, while cells with overlapping ON and OFF regions and modulation values below 1.0 were classified as complex. Hypercomplexity existed more or less in both groups of cells and was shown by the strength of end-stopping on length summation curves [see Fig. 4(E)].

RESULTS

These results are based on measurements obtained from 242 cells in the striate cortex of 19 cats. 134 (55.4%) of the cells were classified as simple and 95 (39.2%) as complex, according to the criteria described in Methods. There were 13 (5.4%) cells which could not be unambiguously classified. A complete set of measurements for each cell consists of up to 12 or more different tests and required a total of 2–3 hr. We were able to complete the entire experimental protocol with only a proportion of cells: for most cells, a sub-set of the total possible measurements was obtained. All the neurons had their RFs centred within 10 deg of the area centralis.

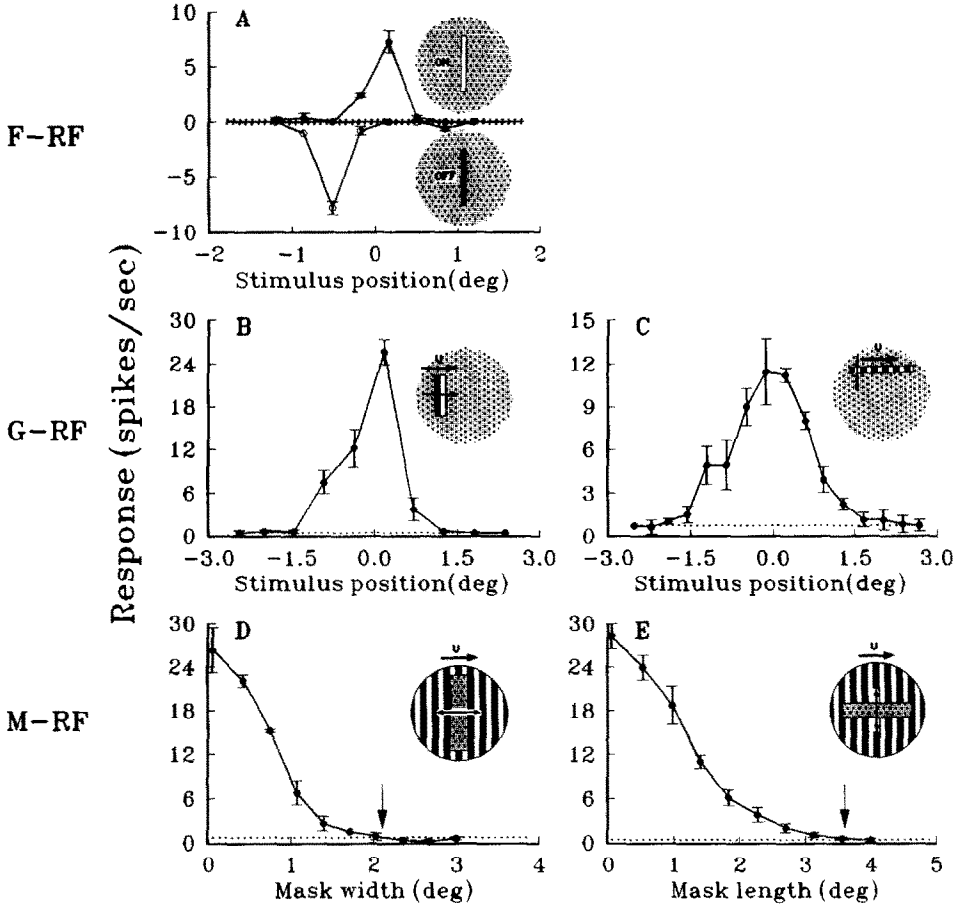

FIGURE 1. Responses of a striate simple cell showing three methods used to determine the extent of classical RF. 1. Flash-bar determined RF (F-RF): (A) shows the response profile of the cell to a flashing light bar and dark bar across the RF. ON- and OFF-regions explored by the light and dark bars are shown upwards and downwards, respectively. Luminance of light bar 22 cd/m^2, dark bar 5.0 cd/m^2, background 8.3 cd/m^2. Bar size 0.3 × 5.0 deg. Position "0" on abscissa represents the centre location of the RF. 2. Grating-patch determined RF (G-RF): (B, C) response profiles of the cell obtained by sweeping a narrow (1.0 deg) sine-wave grating patch along the width axis [inset in (B)] and a short (1.0 deg) grating patch along the length axis [inset in (C)] of the RF. The grating patches were set at the optimal orientation and spatial frequency and drifted in the preferred direction with a speed of 7.8 deg/sec. 3. Masking-patch determined RF (M-RF): (D, E) the response-elimination curves of the cell obtained by masking the RF with a rectangular homogeneous field (8.3 cd/m^2) of increasing dimensions. Beyond this masking area is a background grating of optimal stimulus parameters drifting continuously over the entire stimulus screen. Response amplitude decreased gradually when increasing width (D) or length (E) of the masking. Arrow above the curve indicates the limit of the RF width (D) or length (E). Horizontal dotted lines represent spontaneous discharge rates, error bars represent means ±1 SEM (same for the following figures).

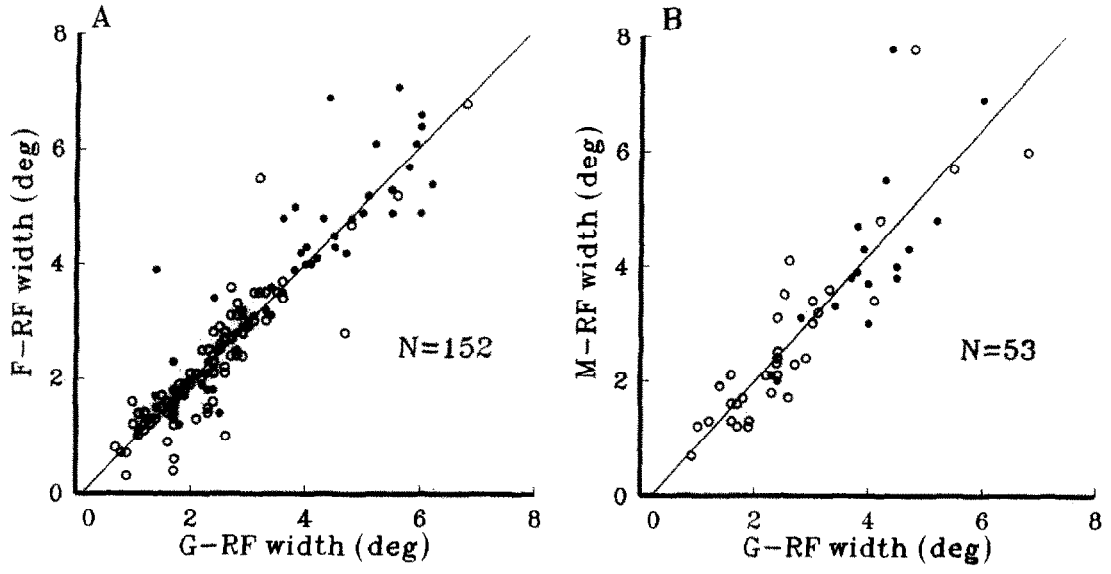

FIGURE 2. Comparisons of RF extent measured by different testing procedures. Each point represents one cell. Open circles denote simple cells, solid circles denote complex cells. (A) Width of G-RF is compared to width of F-RF for 152 cells. (B) Width of M-RF is plotted against width of G-RF for 53 cells. The oblique lines (solid) are regression lines of the data points [(A) slope = 1.03, $r = 0.92$, $P < 0.001$; (B) slope = 1.11, $r = 0.87$, $P < 0.001$].

Quantitative determination of the dimensions of the conventional RF

For the purpose of the present study, it was very important to determine the precise limits of the RF. We did this as accurately as possible using three tests: (1) the plots of ON- and OFF-responses evoked by alternately flashing light and dark bars across the RF (F-RF) [Fig. 1(A)]. This conventional mapping procedure, however, is limited by the weak responses shown by many cells, and was used in this study only for the determination of RF width; (2) the response profiles obtained by placing a sine-wave grating patch at successive positions across the CRT screen, and measuring the response to its drift. The grating was set at the optimal orientation and spatial frequency and drifted in the preferred direction with a speed of 2–4 c/sec (G-RF) [Fig. 1(B, C)]. With stimulus movement along the width axis, usually a complete cycle of the grating was used and an appropriate stimulus length had to be selected for each cell. This test is more sensitive than the F-RF test [compare the peak amplitudes of the profiles in (B) and (A) obtained from the same cell], as optimal stimulus parameters were adopted and spatial summation within the RF was involved. In addition, using a short length grating patch [see inset in Fig. 1(C)] and changing the stimulus positions along the length axis, the length profile of the RF of the cells could also be efficiently determined; (3) the response elimination by masking the receptive field with a rectangular homogeneous field (luminance 8.3 cd/m^2) of increasing dimensions while a background grating of optimal stimulus parameters drifted continuously over the whole CRT screen. In this test, response amplitude decreased gradually with increasing extent of masking [Fig. 1(D, E)]. To determine the dimensions of the RF width, the length of the masking was kept constant and the width was varied randomly under computer control [see inset in Fig. 1(D)]. A similar procedure was used to determine the length of the RF [see inset in Fig. 1(E)]. The responsive region so defined (M-RF) was judged by the point at which the response curve meets the baseline of spontaneous activity of the cell [arrow in Fig. 1(D, E)]. We relied on the M-RF procedure to determine the required size of the central grating when surround tuning properties were investigated (below).

RF extent measured by different methods is compared in Fig. 2. Open circles represent simple cells, solid circles, complex cells. In Fig. 2(A), RF width determined by F-RF is plotted against that determined by G-RF for each individual cell. The comparison shows that the receptive field extent determined by G-RF is in good agreement with that revealed by F-RF measurement (linear correlation obtained with the least squares method, slope = 1.03, $r = 0.92$, $P < 0.001$). At the initial part of the plot, however, most of the open circles fall below the diagonal, indicating that for the simple cells having small receptive fields (< 3 deg in width) the extent measured by G-RF could be broader than that measured by F-RF. A little more than a third of the cells, i.e. 37.2% (90/242), which are not included in the plot, showed either no or very weak response to flashing bars, but vigorous response to drift gratings. In B, G-RF width is compared to M-RF width for 53 cells. A significant correlation is observed between the two measurements (slope = 1.11, $r = 0.87$, $P < 0.001$).

Determination and classification of the IF by length and width summation

The IFs were studied in a total of 149 striate neurons, of which 87 were simple cells, 62 complex cells. For length and width summation, we typically presented drifting grating patches of optimal orientation and spatial frequency to the unmasked RF, varying the

widths (when the width of the IF was measured) or lengths (when the length of the IF was measured). When the RF centre had been precisely determined, the test program was started. The computer presented a series of grating patterns of various lengths or widths in random sequence, each pattern being centred on the RF centre [see insets in Figs 3(A) and 4(A)]. It was crucial for this experiment that the stimulus was of optimal length when IF width measurement was taken and of optimal width for IF length measurement. Since the entire experiment for each cell was relatively long, we re-determined the centre location at the end of the entire experimental series. If the alignment of the centre did not coincide with the initial determination, the data were discarded.

(A) Spatial integration over the width dimension. Figure 3 shows the three types of variations in width-summation properties: facilitatory, inhibitory and disinhibitory integration. In the group data below [Fig. 3(D–F)], those data from simple cells are represented by solid curves, those from complex cells by dotted curves. Since no significant differences were seen between simple and complex groups [see also Fig. 4(D–F) for length integration], the data are pooled for further analysis.

Representative examples of the three variations are shown in Fig. 3(A–C). To compare the width of IF with the width of the conventional RF in individual neurons, the RF width determined by F-RF (pointed by hollow arrow), G-RF (by solid arrow) and M-RF (the zero-response point on the curve) tests, respectively, along the RF width axis are shown in the same plots. The IF was usually several times wider than the RF for most of the cells tested [for group data, see Fig. 6(C)].

For the cells we examined, 33 of 122 (27.1%) showed *facilitatory integration* over the width dimension; the results of 12 such cells are illustrated in Fig. 3(D). With an increased width of the stimulus grating, the response of these cells increased gradually to their maxima over varying ranges beyond the classical receptive field and were then maintained at this level. Figure 3(E) illustrates *inhibitory integration* for 19 cells: the total number of this type of cell was 77 (63.1%). For these cells, a peak point was reached within a certain range, and then the response decreased to various extents with increasing grating widths. Inhibition was sometimes strong enough to reduce the cell activity to complete silence. This feature of simple and complex cells has been labelled the "inhibitory sideband" by Bishop *et al.* (1973) and "side stopping" by De Valois *et al.* (1985) in simple and complex cells. As was reported for retinal ganglion cells and lateral geniculate neurons (Li & He, 1987; Li *et al.*, 1991, 1992), a *disinhibitory integration* field was observed in 12 (9.8%) striate cells from our sample. For these neurons, a drop in response was seen when the grating patch exceeded the optimum width, but a still further increase in stimulus width revived the response by a

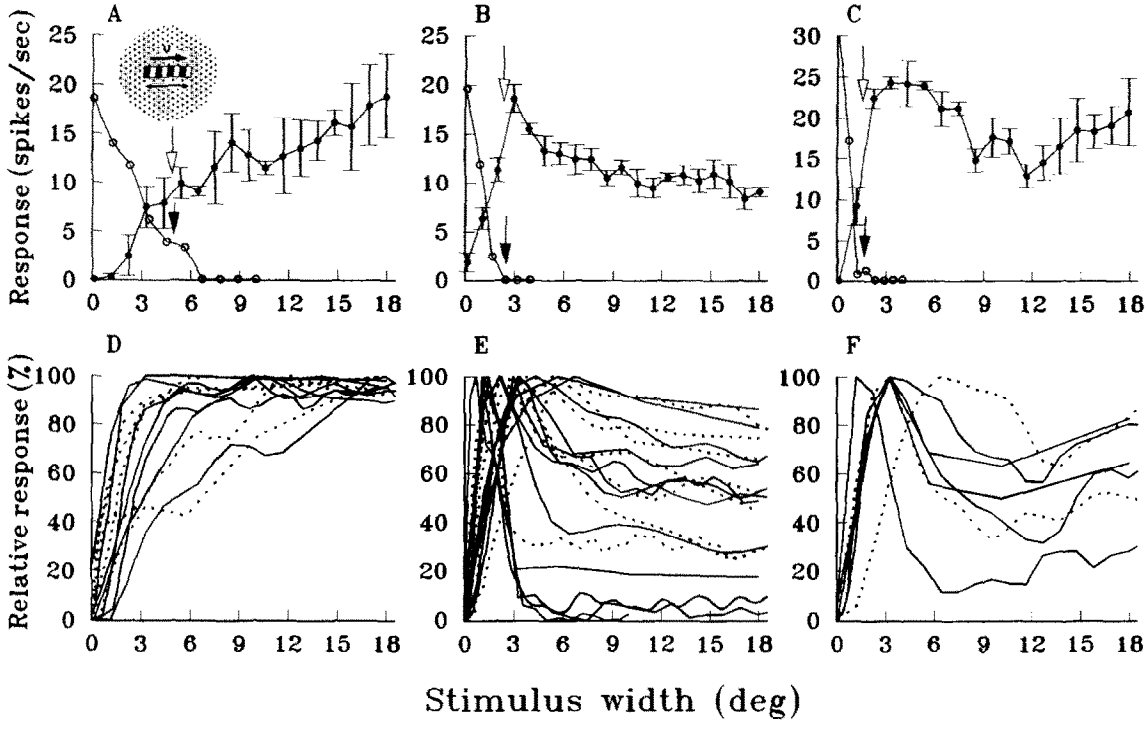

FIGURE 3. Three types of width integration properties. Stimuli were sine-wave grating patches with optimal orientation and spatial frequency, but varying in width [see inset in (A)], all centred on the RF centre and drifting continuously in the preferred direction. Responses were accumulated for 10 cycles and standard errors were calculated over five repetitions (error bars, ±1 SEM). (A–C) Three representative cells showing facilitatory, inhibitory and disinhibitory integration, respectively. Width of the classical RF for each cell is also shown for comparison; open arrows point to the limit determined by F-RF, solid arrows the limit of G-RF, and the descending curve at the left of each plot represents extent of M-RF of each cell. (D–F) More examples of the three types of integrations, (D) facilitatory, (E) inhibitory, (F) disinhibitory. Data from simple cells are illustrated by solid curves, those from complex cells by dotted curves. The response amplitudes of the cells were normalized.

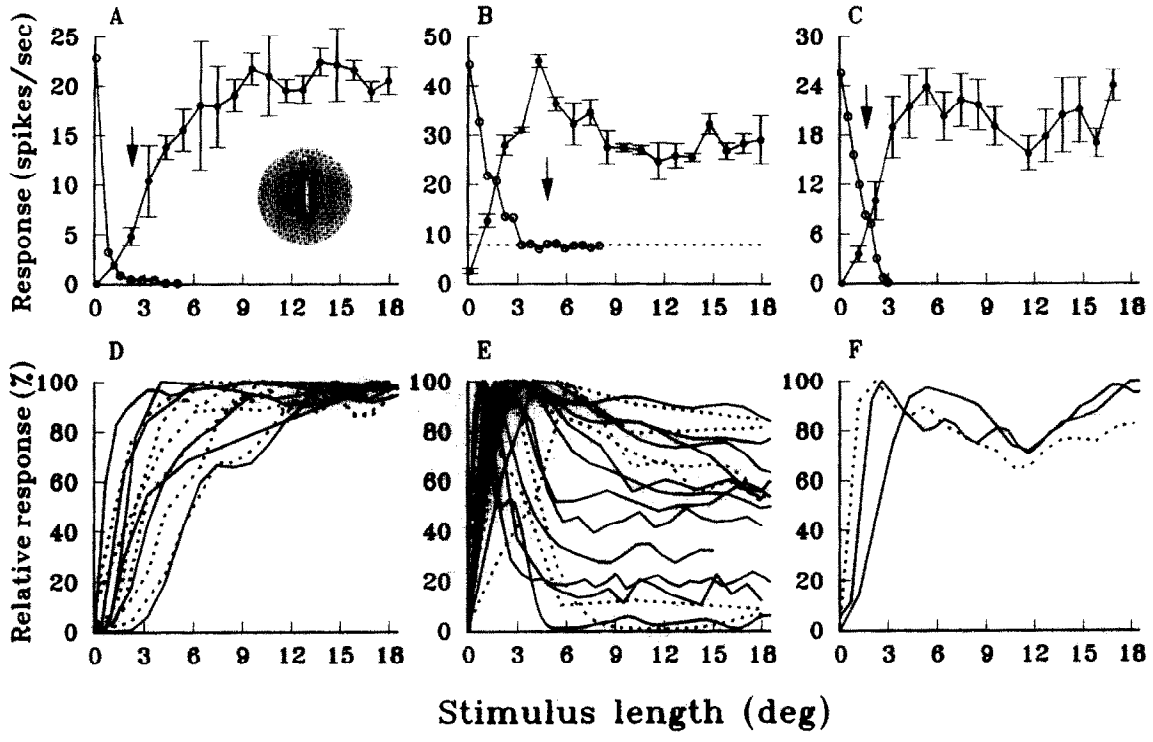

FIGURE 4. Three types of length integration properties. Stimuli were principally the same as in Fig. 3, but varied in length [see inset in (A)]. (A–C) Individual examples of facilitatory (A), inhibitory (B) and disinhibitory (C) integrations, respectively. Arrow indicates the length of G-RF, and the descending curve, the length of M-RF for each cell. (D–F) More examples of the three types of integrations. Solid curves, simple cells; dashed curves, complex.

greater or lesser amount. Seven of these cells are illustrated in Fig. 3(F).

(B) Spatial integration over the length dimension. In Fig. 4(A–C), three representative length–response curves illustrate the same three variations in length integration seen previously for width. In comparison with the length of the classical RF shown by G-RF and M-RF tests (F-RF test was not successfully used for RF length determination), the integration field was seen beyond the ends of the RFs. Of 122 cells tested, 45 (36.9%) showed facilitatory length integration [Fig. 4(A, D)], 68 (55.7%) showed inhibitory length integration [Fig. 4(B, E)], and the remaining 9 (7.4%) were disinhibitory [Fig. 4(C, F)]. A set of typical cells for each group is shown in Fig. 4(D–F). From Fig. 4(E), it can be seen that "end-stopping" is present to a greater or a lesser extent in both simple and complex cells.

The results fit well with earlier studies on the length–response curves of area 17 cells using moving bars as the stimulus. Rose (1977) illustrated both facilitatory and inhibitory flanks beyond the classical receptive field, and Orban, Kato and Bishop (1979) observed these two types of surround effects, referring to them as "end-free" and "end-stopped", respectively. Their frequencies of occurrence are also similar to those observed in the present study.

(C) Different combinations of length and width integrations. Width and length integration for a given cell could be different or similar. Taking only facilitatory and inhibitory types into consideration (95 cells), all four possible combinations of length and width integration were found. These may be expressed as (1) L+, W+; (2) L−, W−; (3) L+, W− and (4) L−, W+ where L and W represent the length and width dimension, and the signs "+" and "−" facilitatory and inhibitory integration, respectively. Examples of each of the four combinations are illustrated in Fig. 5. Sixteen cells (16.9%) showed the first combination [L+, W+; Fig. 5(A)], they tend to integrate stimulus patterns of a similar orientation and spatial frequency over an extensive area. The second combination [L−, W−; Fig. 5(B)] was shown by 46 cells (48.4%): they exhibited inhibition beyond both the ends and sides of the RF. This type of combination produces an optimal response to a restricted local stimulus, and may play a role in border and corner enhancement for textured patterns. The third type of combination (L+, W−) (23 cells, 24.2%) exhibiting inhibition beyond the two sides of the RF (side inhibition), but facilitation along the length axis [Fig. 5(C)], may result in a preference for elongated patterns. We measured area–response functions in seven L+/W− cells using circular gratings of increasing diameters. All showed inhibitory integration as the stimulus grating extended beyond the sides and ends of the classical RFs. There were only 10 cells (10.5%) in the fourth group (L−, W+), that showed inhibition beyond the ends of the RF and facilitation along the width dimension [Fig. 5(D)]. Those cells that possessed strong end-inhibition correspond to the hypercomplex types of Hubel and Wiesel (1962, 1965).

(D) The extent of the IFs. The extent of the IFs of striate cortex neurons was evaluated from the width- and

length-summation curves from the point at which the curve reached its maximum and remained constant (for the facilitatory and disinhibitory integration groups) or at which the response decreased to its minimum and began to level off (for the inhibitory integration group). Figure 6(A, B) illustrates the distribution of the range of IFs in the width and length dimension, respectively, for a population of 122 cells. No apparent peak was seen in the distribution of histograms for either width or length, when the extent of the IFs was represented by degree of visual angle. The width and length distributions illustrate that, for about 70% of the cells in our sample, IFs were >6 deg; some were extended beyond the limit of the stimulus screen (>18 deg). To make an estimate of the relative size of IF to RF for each individual cell, we replotted the distributions in Fig. 6(C, D) as the ratio IF/RF. A clear maximum occurs around a ratio of 3. The IFs in more than 70% of the cells were 2–5 times the size of their RF; in about one-quarter of the cells, more than five times. This finding is in agreement with the previous studies of Maffei and Fiorentini (1976).

Tuning properties of the IFs

Do cortical IFs show tuning properties and if so, are their properties similar to the tuning of their RFs? Since no direct response can be elicited by stimulating the IF alone, we had to present a conditioning stimulus, i.e. an optimally oriented grating patch covering the entire excitatory RF, to drive the cells continuously. As the M-RF test may detect any possible contaminating responses from the excitatory area, we took it to be the most reliable measurement in deciding the diameter of the central grating. The tuning properties of the IF were tested using a peripheral concentric grating whose inner diameter was equivalent to or slightly larger than the longer axis (width or length) of the excitatory RF under study [see inset in Fig. 13(A)]. The parameters of the central and peripheral gratings were adjusted separately by computer. The amount of facilitation and inhibition was revealed as an increase or reduction in the cell activity elicited by the always optimal central stimulus, while the surround grating changed in orientation, spatial frequency or direction and speed of movement.

(A) Spatial frequency tuning. The spatial frequency tuning of the conventional RF was first obtained by plotting the response amplitude of the cell against the spatial frequency of the central grating while the surround was uniformly illuminated (thin curves in Fig. 7). Then, using the central grating as the conditioning stimulus, the spatial frequency tuning of the IF was determined by the variations in the maintained discharge it produced against the spatial frequency of the peripheral gratings (bold curves in Fig. 7). During the test, both the central and surround gratings were set at the optimal orientation and preferred direction of the cell. We examined the IFs of 29 cells in this domain; 23 revealed clear selectivity for spatial frequency. Of these, 21 showed an inhibitory effect and two facilitatory effect.

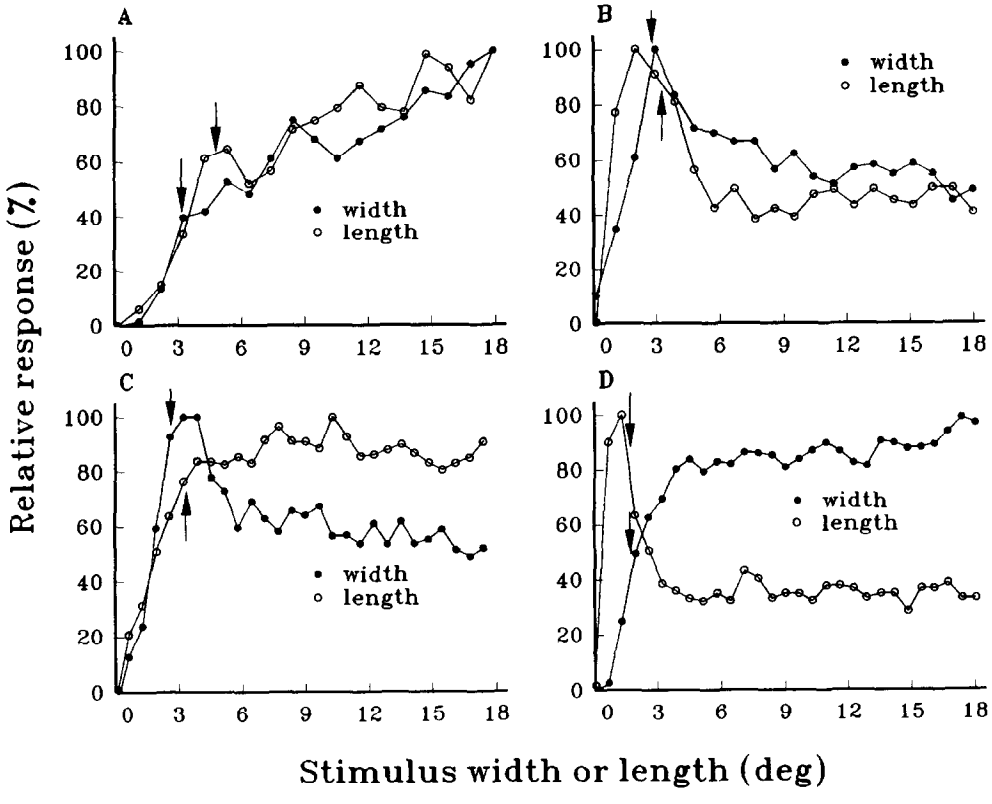

FIGURE 5. Length- and width-response curves of four simple cells showing different combinations of length and width integrations. (A) Both the length and width integrations are facilitatory; (B) both are inhibitory; (C) length integration facilitatory, width inhibitory; (D) length integration inhibitory, width facilitatory. Arrows indicate the length and width of the G-RF of each cell.

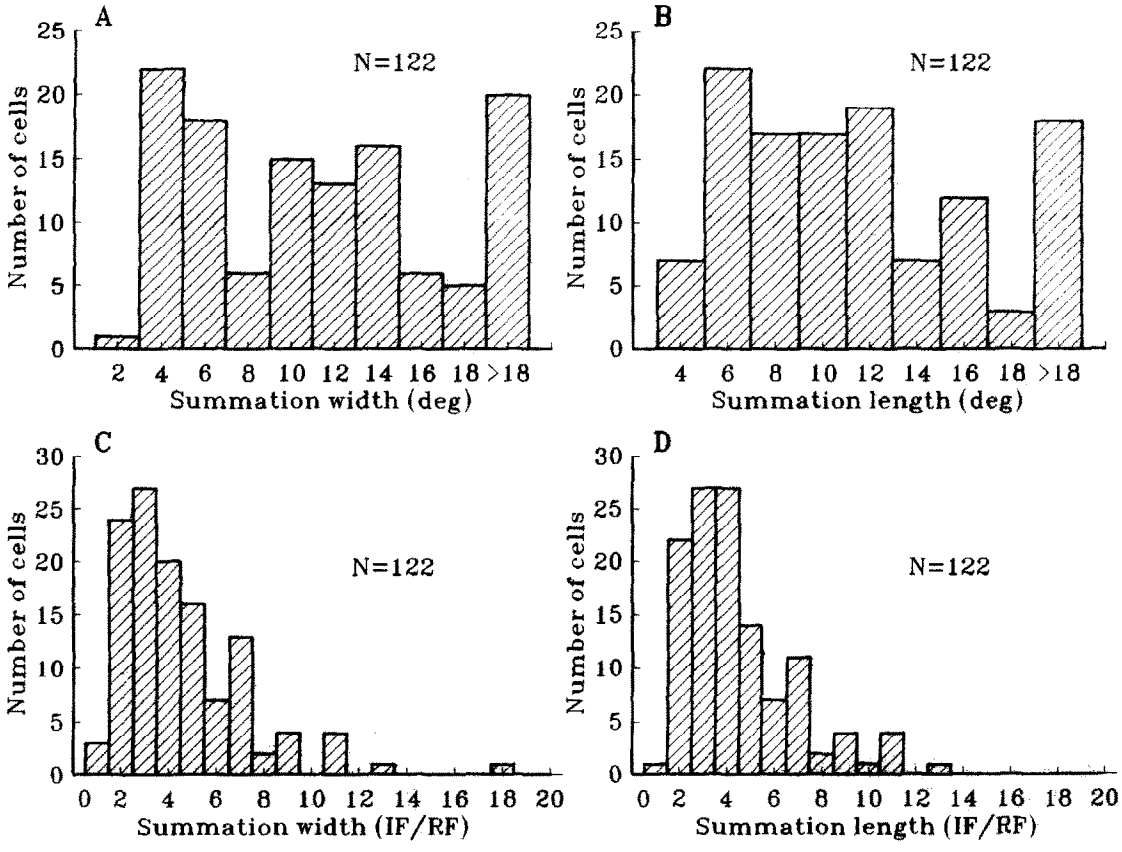

FIGURE 6. Distribution histograms of the extent of the integration fields of 122 striate cortex cells. In (A) and (B) width and length of the integration fields are represented by degrees of visual angle, and in (C) and (D) by the relative size of IF to G-RF for individual cells (ratio IF/RF).

Figure 7 shows how the inhibitory and facilitatory effects of the surround grating depend on spatial frequency. The spatial frequency tuning function of the IF (dark curve) is compared directly with the tuning function of the RF (thin curve) for each of the four cells. The mean firing rate elicited by the centre stimulation alone (the surround was a uniform field) is indicated by a horizontal dashed line, which was measured repeatedly in the intervals between test trials. The control level thus obtained was sometimes lower than the excitatory tuning peak, because of the parameter-specific adaptation caused by the long-lasting, central grating (Movshon & Lennie, 1979; Marlin, Hasan & Cynader, 1988). For comparison, the amplitude of the centre excitatory tuning curve is normalized to this level at its peak (also for similar plots shown later). For the complex cell shown in Fig. 7(A), the shape of the spatial frequency tuning curve of IF is roughly a mirror image of that of the RF and with approximately the same peak position (0.37 and 0.42 c/deg for RF and IF, respectively) and bandwidth. For the simple cell shown in Fig. 7(B), the situation is quite different. In this case, maximal inhibition of the surround occurred at a spatial frequency (0.23 c/deg) far below the optimal spatial frequency of the RF (0.54 c/deg). We also observed cells for which the maximal inhibition of IF occurred at spatial frequencies higher than the optimal spatial frequency of the RF [see Fig. 8(A)]. The simple cell in Fig. 7(C) shows similar peak positions (0.46 and 0.48 c/deg) in the IF and RF spatial frequency tuning curves, but the inhibition (IF) curve has a much broader bandwidth than the excitation (RF) curve, so that spatial frequencies which are far beyond (higher than) the excitatory bandpass still elicit strong inhibition. Only two cells in this sample showed facilitatory surround effects; the spatial frequency tuning functions of one such cell (simple) are shown in Fig. 7(D). For this cell, IF and RF tuning curves had about the same bandwidth, but slightly different maxima (0.21 and 0.30 c/deg). Although the surround facilitation was tuned somewhat similar to that of the classical central response, it cannot be an artefact due to stimulation resulting from the surround grating on the central, RF excitatory mechanisms. As was described above, in all tuning experiments, the boundary of the central excitatory field was determined by the masking procedure, which may exclude any possible encroachment of the centre response. In addition, the inner diameter of the surround grating used was usually larger than the actual size of the RF under investigation. For the cell shown in Fig. 7(D), the M-RF was 7.8 × 5.5 deg, and the inner diameter of the surround grating used was 11 deg. This may also explain the low amplitude of the surround facilitation for this cell.

To look more precisely at the relationship between IF and RF tuning properties, the optimal spatial frequency and bandwidth of the IF curve were compared to those of the RF for individual cells. In Fig. 8(A) are plotted the optimal spatial frequency of the IF (the spatial

frequency of surround grating which elicited maximum inhibition or facilitation) of each cell against the optimal spatial frequency of its RF. Although there is considerable variability, the scatter plot illustrates a significant correlation between the optimal spatial frequencies of IF and RF ($r = 0.70$, $P < 0.001$). Only in a minority of the cells were the optimal spatial frequencies for IF and RF significantly different [Fig. 7(B)]. For these cells, the displaced tuning peaks for the excitatory and inhibitory mechanisms may enhance contrast in the spatial frequency domain.

In Fig. 8(B) we compare the bandwidth of the spatial frequency tuning curve (taken as the bandwidth at the half amplitude) of the IF to that of the RF for individual cells. All the points are above the diagonal, indicating that the bandwidth of IF tuning is to a greater or lesser extent wider than that of the RF. For some cells, the broadening of the IF tuning was observed predominantly on one side (the lower or the higher frequency side), and for others, equally at both sides. This broadly tuned surround inhibition would serve to sharpen spatial frequency tuning curves by reducing the flanks.

(B) Speed tuning. We tested speed tuning of the IFs for 20 cells, 14 out of which showed clear speed selectivity. First we determined the speed tuning of the RF with the central grating at the optimal orientation and spatial frequency for the cell. To test the speed selectivity of the IF, both the central and surround gratings were set at optimal values of orientation, spatial frequency and movement direction, but the movement speed of the surround grating was varied progressively. In Fig. 9 cell response was plotted as a function of movement speed of the surround grating, and the speed tuning of the IF (bold curves) was compared to that of the RF (thin curves) in two cells. In Fig. 9(A), the cell was inhibited maximally as the surround grating drifted at speeds close to the peak of the centre speed tuning curve. The speed tuning curves of IF and RF had similar shape and bandwidth; both showed a steeper variation in response amplitude at the low-speed side and a much gentler cut-off at the high-speed side. The IF and RF of the cell in Fig. 9(B) are tuned to about the same peak value (7 and 8 deg/sec, respectively), but the IF curve showed a second inhibitory peak at 27 deg/sec and a much higher cut-off speed than the RF, which may provide a neuronal mechanism for discriminating speed contrast between the centre and surround areas. The speed interactions between centre and surround are likely to be

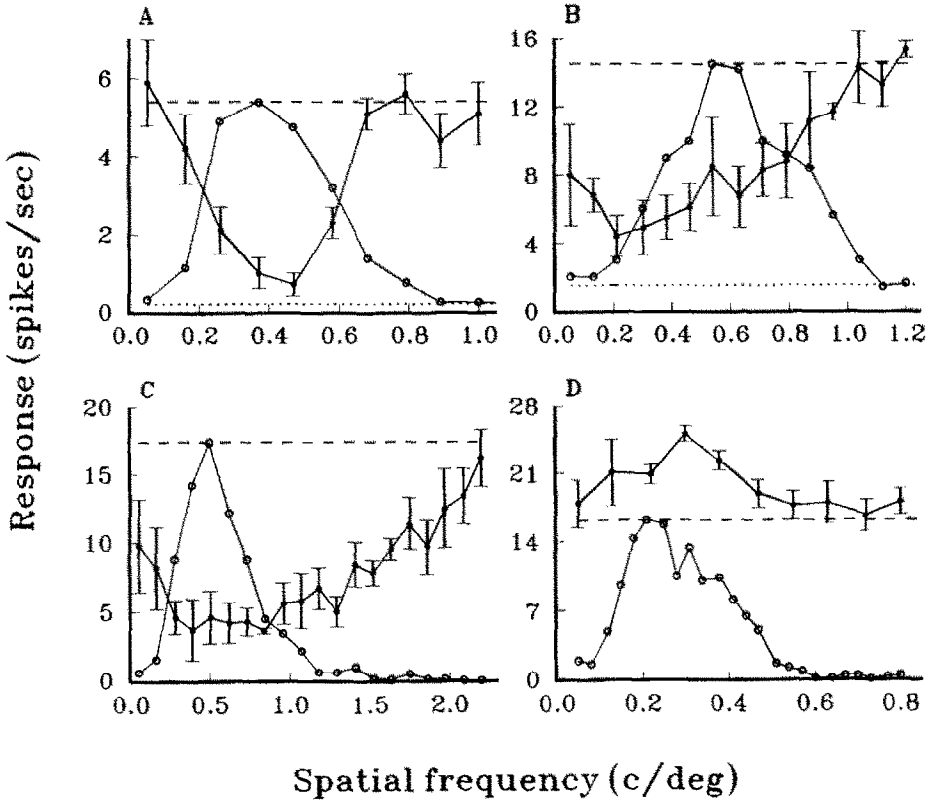

FIGURE 7. Spatial frequency tunings of the integration fields and of the related receptive fields of four striate cells. (A) Complex cell, G-RF 4.7 × 5.7 deg, IF 10.1 × 18 deg (the first panel indicates the width and the second the length of RF and IF, same for the following panels), W−/L− type. Central grating dia 6 deg. (B) Simple cell, G-RF 1.7 × 2.5 deg, IF 8.5 × 5.2 deg, W−/L− type. Central grating dia 2.5 deg. (C) Simple cell, G-RF 1.6 × 1.6 deg, IF 18 × 18 deg, W−/L−. Central grating dia 3.5 deg. (D) Simple cell, G-RF 4.8 × 3.2 deg; IF 18 × 16.2 deg, W+/L+. Central grating 11.0 deg. The bold curves show tuning of the IFs and the thin curves tuning of the RFs. The IF tuning was determined by a surround grating in the presence of a conditioning central grating [see inset in Fig. 13(A)]. Both gratings were optimally oriented, grating contrast was 0.3. Dashed horizontal lines indicate the mean discharge rates elicited by the conditioning centre grating alone when the surround was uniformly illuminated. The RF tuning curves are normalised to this level at the peak point (same for the following figures).

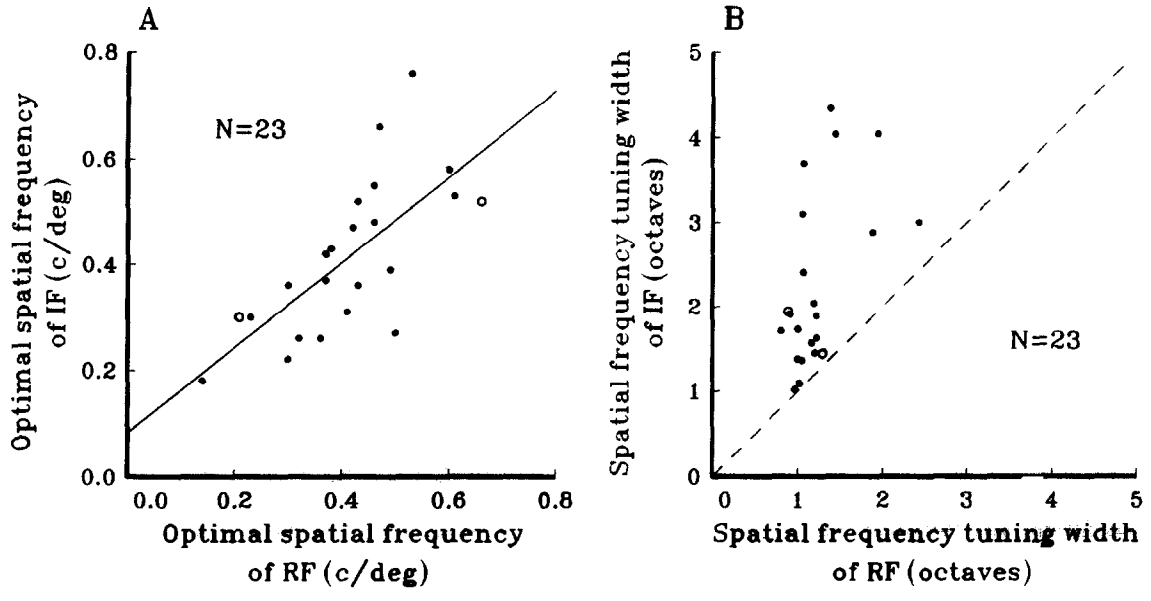

FIGURE 8. Comparison of spatial frequency tunings of IF and RF for 23 striate cells. Cells showing facilitatory surround effect are denoted by open circles, those showing inhibitory surround effect by solid circles. (A) Optimal spatial frequency of RF is plotted against optimal spatial frequency of IF. The oblique solid line is regression line (slope = 0.80, $r = 0.70$, $P < 0.001$). (B) Spatial frequency tuning width of IF is compared to that of RF. Points above the diagonal line (dashed) indicate cells whose spatial frequency tuning width of IF is broader than the RF's tuning.

the substrate, at the cellular level, for mechanisms of contrast illusions of movement speed (see Discussion).

In Fig. 10(A), are plotted the optimal speed of the IF of each cell against the optimal speed of its RF for the 14 cells examined. A significant correlation ($r = 0.78$, $P < 0.001$) is shown between them, indicating that, for most cells, IF and RF were tuned to similar optimal speed. In Fig. 10(B), bandwidth (at half amplitude) of the speed tuning curve of IF is compared to that of RF for individual cells. It can be clearly seen that, for most cells, the bandwidth of IF tuning is wider than the RF's tuning. As has been described for spatial frequency tuning, the differences in bandwidth of IF and RF tuning curves might serve to improve speed selectivity.

(C) Orientation/direction tuning. As orientation/direction selectivities are the most striking features for cortical neurons, we placed our emphasis on investigating the orientation/direction tuning properties of the IFs. Since this tuning property was determined with moving gratings and the direction of stimulus movement was always perpendicular to the long axis of orientation, the tuning property thus determined reflects a combination of both orientation and direction components. Therefore, the two parameters in this paper were analysed together. The term "direction" alone is used if the responses of the cells to two opposing directions of movement are compared.

We first determined the orientation/direction tuning of the RF using the central grating patch (at the optimal spatial frequency), as in the above experiments. Then the

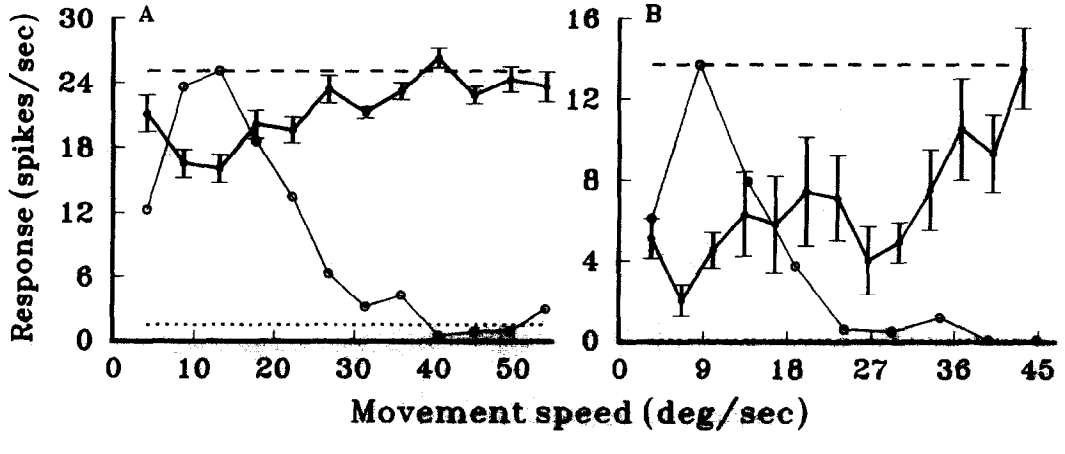

FIGURE 9. Speed tuning of the IF (bold curve) and of the related RF (thin curves) of two simple cells. (A) The cell has a G-RF of 4.7 × 4.7 deg, IF 16 × 10 deg, W−/L−. Central grating dia 5 deg. (B) G-RF 2.9 × 2.6 deg; IF 12.8 × 3.9 deg, W−/L−. Central grating dia 4.1 deg. Both centre and surround gratings were of optimal spatial frequency and drifted in the preferred direction of the related cells.

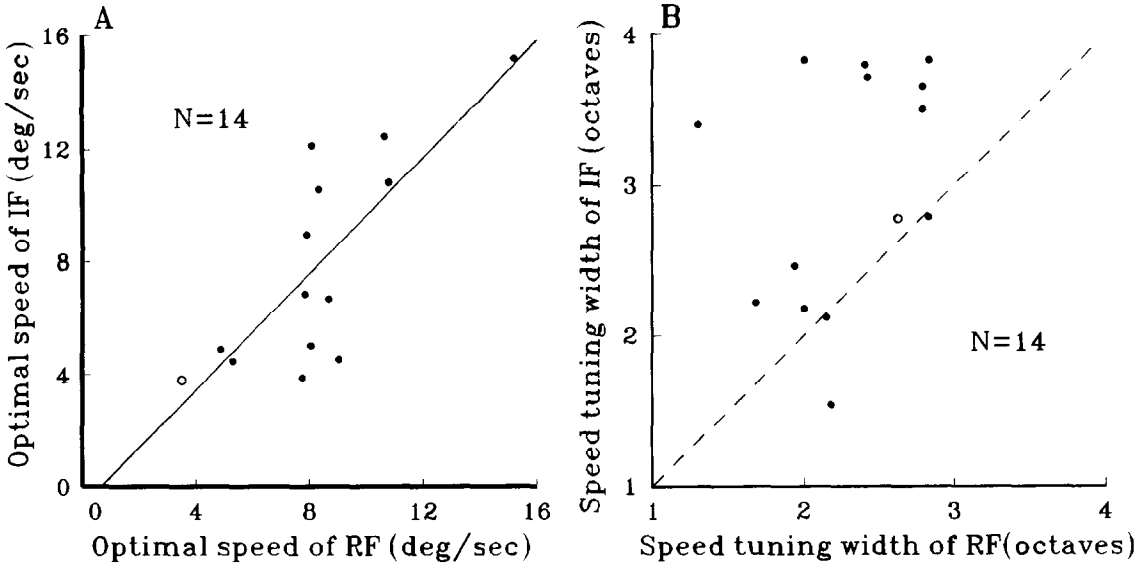

FIGURE 10. Comparison of speed tuning of RF with speed tuning of IF for 14 striate cells. One cell showed facilitatory surround effect (open circle), the others (solid circles) showed inhibitory surround effect. (A) Optimal speed of RF is plotted against optimal speed of IF. The oblique line (solid) is regression line (slope = 1.03, $r = 0.78$, $P < 0.001$). (B) Speed tuning width of RF is compared to speed tuning width of IF. Points lying above the diagonal line (dashed) indicate cells whose IF is tuned to a broader range of speed than their RFs.

central grating was maintained at the optimal orientation and preferred direction to activate the cell continuously, and the peripheral grating, having identical spatial frequency and movement speed to the centre, was presented at the surround and rotated randomly between 0 and 360 deg using 10–20 deg intervals. We investigated the orientation/direction dependence of the surround effect in 47 striate cells, of which 42 (24 simple, 18 complex) were orientation or orientation and direction selective. Although the effect of the orientation of the surround stimulus on the centre response varied from cell to cell, three types of surround tuning properties were identified. (a) *Peak-inhibitory surround* 73.8% of the cells (31/42) showed maximal inhibition when surround grating matched the optimal orientation of the RF and little or no effect when the surround grating was oriented beyond the optimal range. (b) *Peak-facilitatory surround* 16.7% of the cells (7/42) showed maximal facilitation when the surround grating matched the optimal orientation of the RF. (c) *Inhibitory/facilitatory surround.* Four cells in this sample (9.5%) exhibited maximal inhibition when the optimally oriented surround grating drifted in one direction, and maximal facilitation when it drifted in the opposite direction.

Typical examples of the peak-inhibitory surround are shown in Fig. 11(A, B). For the cell shown in Fig. 11(A), the orientation tuning curve of RF (the thin curve) peaked at the 54/−126 deg axis (the two orientations differing in 180 deg from each other were at the same orientation, but drifted in opposite directions). Similar peak locations (49/−131 deg) but wider bandwidth were shown for its surround tuning curve (bold curve). Figure 11(B) shows another example. The RF tuning of the cell peaked at −180 deg and the surround peaked at the −176/4 deg axis. For this cell, a somewhat facilitatory type of effect was seen at the non-optimal orientations.

An example of a peak-facilitatory surround is shown in Fig. 11(C). The cell was narrowly tuned and optimally oriented along the 52/232 deg axis. Its surround tuning showed a facilitatory narrow peak at an orientation (48/228) very close to the centre peak. The facilitated response at peak orientation was 69% greater than the response to the central grating alone. In this type of neuron, inhibition was always seen at non-optimal orientations. In some cases, as for example in Fig. 11(D), no periphery effect was seen at the optimal orientation, but strong inhibition was elicited when the surround grating was set at non-optimal orientations. This is known as "cross-orientation inhibition" in the literature. In both Fig. 11(C, D), the strongest inhibition was observed at each side of the facilitatory peak. For the cell in Fig. 11(C), the response at the inhibitory side band (71 deg) was reduced by 86%, and in Fig. 11(D) by 90% (at 281 deg). The facilitation at the optimal orientation, in combination with the strong inhibition at adjacent but non-optimal orientations, would greatly improve the orientation selectivity of the cell.

In Fig. 11(E, F) are shown two examples of the facilitatory/inhibitory surround effect. For these cells, the two peaks in the surround tuning curves were of opposite polarities. For the cell shown in Fig. 11(E), one peak (30 deg) close to the cell's preferred direction is facilitatory, the other in the opposite direction (−150 deg) showed an inhibitory effect. This indicates an enhancement of cell activity when the centre and surround stimuli moved in the same direction, and suppression when they moved in opposite directions. A complementary type of centre–surround interaction is seen in Fig. 11(F), where the conditioning grating in the

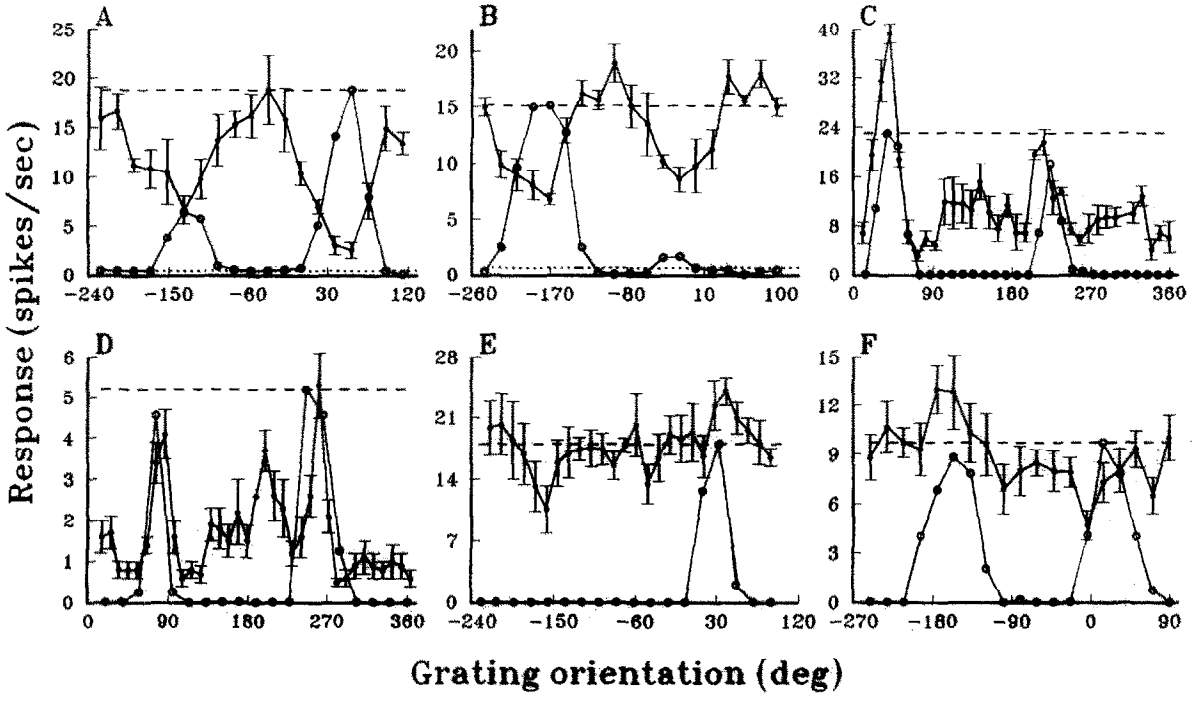

FIGURE 11. Orientation tunings of the IFs (bold curves) and of the related RFs (thin curves) of six striate cells. (A) Simple cell, G-RF 2.4 × 2.4 deg, IF 7.4 × 8.6 deg, W−/L−. Central grating dia 2.6 deg. (B) Simple cell, G-RF 2.3 × 1.9 deg, IF 14.2 × 6.7 deg, W−/L−. Central grating dia 3.0 deg. (C) Simple cell, G-RF 1.6 × 1.3 deg, IF 11.6 × 10.6 deg, W−/L+. Central grating dia 4.5 deg. (D) Complex cell, G-RF 1.7 × 2.0 deg, IF 18.0 × 16.5 deg, W−/L−. Central grating dia 3.0 deg. (E) Simple cell, G-RF 1.4 × 1.4 deg, IF 3.3 × 18.0 deg, W+/L−. Central grating dia 5.0 deg. (F) Complex cell, G-RF 6.0 × 5.0 deg, IF 18.0 × 16.0 deg, W−/L+. Central grating dia 12.0 deg. 0 and 180 deg correspond to a vertical grating that drifts towards left and right, respectively. 90 and 270 deg correspond to horizontal grating drifting upwards and downwards, respectively.

centre was drifted in the 23 deg direction, surround inhibition was seen when the centre and surround gratings drifted in the same direction, and facilitation occurred when they drifted in opposite directions. Note that, in the latter case, the optimal axes of IF (−173/7) and RF (−157/23) are 16 deg apart.

In Fig. 12(A) the relationship between the orientation producing maximal facilitation or inhibition in the surround and the optimal orientation of the centre is shown for 42 cells. Open circles denote cells that exhibited facilitatory surround effects, solid circles denote cells that exhibited an inhibitory surround effect, and open

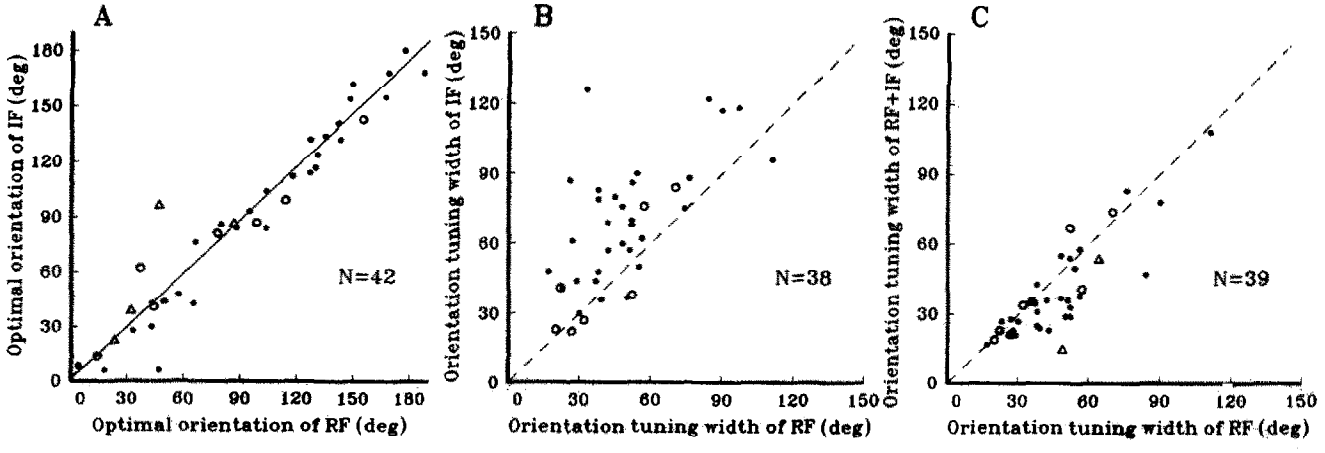

FIGURE 12. Comparison of the orientation tuning property of the IF with that of the RF for a sample of striate cells. Open and solid circles denote cells that exhibited facilitatory and inhibitory surround effect, respectively; triangles represent cells exhibiting inhibitory/facilitatory effect. (A) The optimal orientation of IF for each cell is plotted against the optimal orientation of its RF. Oblique line (solid) is regression line (slope = 0.97, $r = 0.95$, $P < 0.001$). (B) The orientation tuning width of IF is plotted against the orientation tuning width of RF. Most points fall above the diagonal line (dashed), indicating that the IF tunings of the cells are significantly broader than the tuning of the RFs ($t = 5.13$, $P < 0.01$). (C) The orientation tuning width measured by central grating is compared to the orientation tuning width measured by the entire field grating (RF + IF). The tuning width became significantly narrower when both RF and IF were stimulated simultaneously by a broad grating ($t = 3.78$, $P < 0.01$).

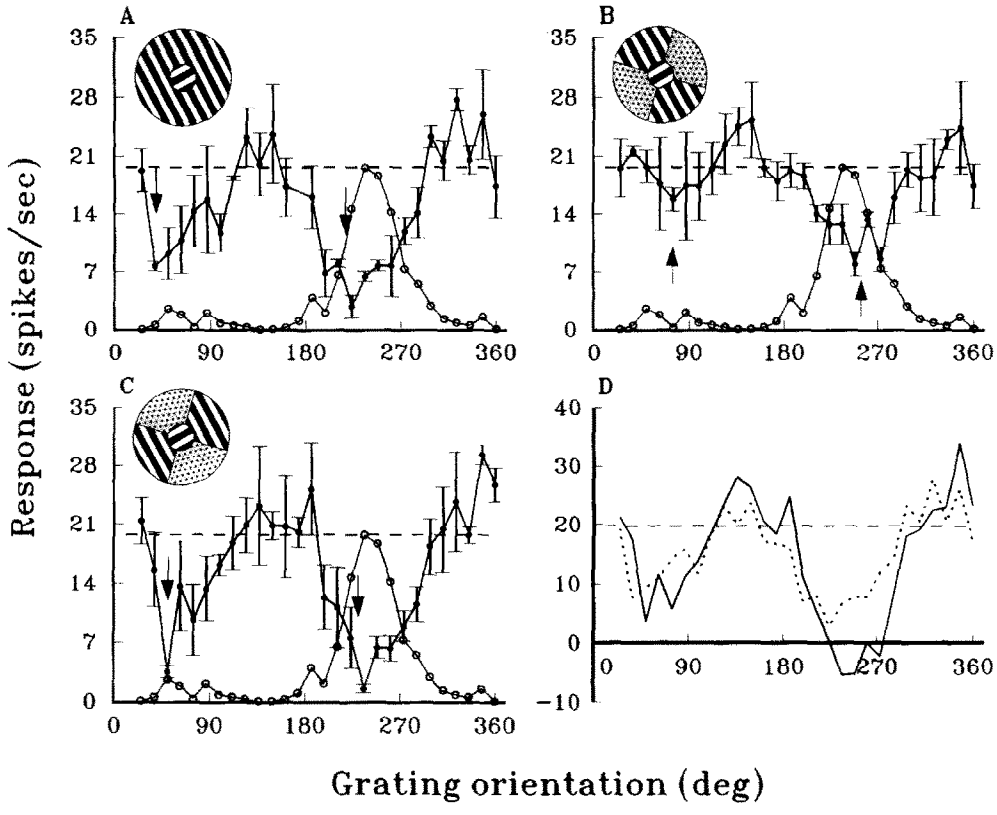

FIGURE 13. Comparison of orientation tuning between the side areas and the end areas of an inhibitory IF. Simple cell, G-RF 2.2 × 1.8 deg, IF 7.6 × 8.2 deg. Both the length and the width integration curves of the cell showed strong surround inhibition. (A) shows the orientation tuning of the entire IF (bold curve) tested by the usual concentric grating patterns (see inset). (B) shows the orientation tuning of the side areas when the end areas are covered by a sectorial masking (see inset). (C) shows the orientation tuning of the end areas when the side areas were masked by the sectors (see inset). (D) compares the tuning curve of the entire surround (dotted curve) with the sum of the end and side tuning curves (solid curve). The diameter of central grating is 2.6 deg. Spatial frequency of the centre and surround gratings is 0.39 c/deg. Drift speed 10.2 deg/sec. Arrows indicate the orientation axes of the IF.

triangles an inhibitory/facilitatory surround. A strong correlation ($r = 0.95$, $P < 0.001$) is seen between the optimal orientations of IF and RF, and the slope of the regression line (0.97) illustrates that the optimal orientation of the surround tends to match the optimal orientation of the RF, with a mean variance of 11.8 deg (SD = 12.7). Only in very few cases were large differences seen between the tuning peaks of the centre and the surround.

In Fig. 12(B) are plotted the orientation tuning width (defined as bandwidth at half amplitude) of IF against that of RF for 38 cells. The four cells showing inhibitory/facilitatory surround effects were not included, because of the weakness of the effect. The results show that the orientation-tuning widths of the IFs are significantly broader than that of the RFs ($t = 5.13$, $P < 0.01$). We also measured the orientation tuning functions for 39 cells when both the RF and IF were simultaneously stimulated with an extended grating (18 deg in dia). In Fig. 12(C) orientation tuning width measured by local RF stimulation (abscissa) is plotted against that obtained from whole field (RF + IF) stimulation (ordinate). It can be seen that most of the points, mainly those representing the cells exhibiting an inhibitory surround effect (solid circles), lie below the diagonal line. This provides evidence that the existence of a more broadly tuned inhibitory surround may sharpen orientation selectivity, i.e. make it significantly narrower ($t = 3.78$, $P < 0.01$), if the stimulated area is wide enough to involve both the RF and the IF.

As can be seen from Fig. 5(B), some cells showed strong end stopping (inhibition beyond the ends of RF) and the same degree of side stopping (inhibition beyond the sides of RF) in their width- and length-summation curves. Does the presence of both end stopping and side stopping in the same striate cortex cell suggest a unitary suppressive region spreading all around the RF? If this is true, the tuning properties over the end and side areas of the IF should be identical. In three such cells, we tested the orientation tuning repeatedly with a sector mask [two opposite sectors made of black cardboard, see inset in Fig. 13(B, C)] covering either the end area or the side area and leaving the other area of the IF (the ends or sides, but not both) exposed to the surround stimulus grating. An example is shown in Fig. 13. The bold curve in Fig. 13(A) illustrates the overall tuning properties of the entire IF when no masking was used. Figure 13(B, C) reveals the orientation/direction tuning of the side and end areas, respectively, by using proper masking. There is a remarkable difference between the end and side

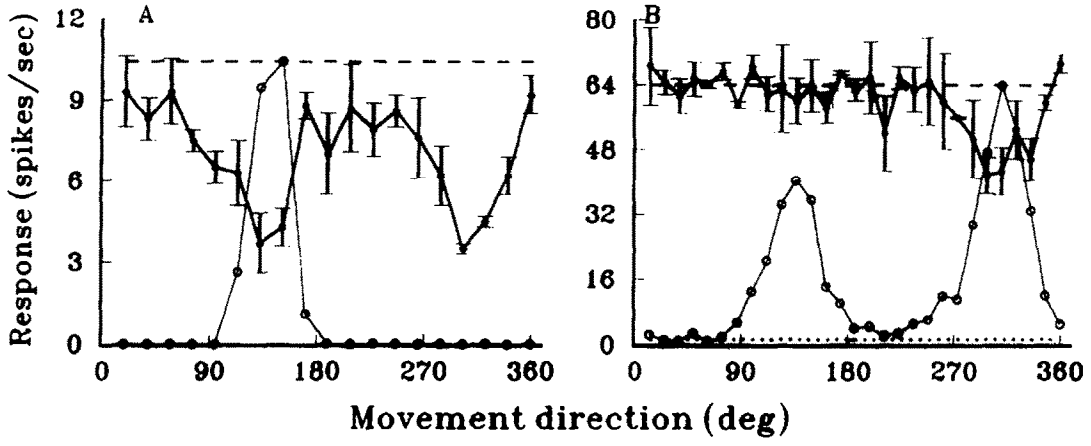

FIGURE 14. Comparison of IF and RF direction selectivities for two striate cells. (A) Simple cell, G-RF 2.5 × 3.5 deg, IF 11.5 × 9.8 deg, W−/L−. Central grating dia 4 deg. Drift speed 10 deg/sec. The RF is highly direction selective, whereas the IF is not. (B) Complex cell, G-RF 3.0 × 2.9 deg, IF 16.9 × 6.4 deg, W−/L−. Central grating dia 5.2 deg. Drift speed 10.8 deg/sec. The RF showed some direction selectivity, whereas the IF showed a complete direction selectivity.

regions in the inhibition around 60 deg. The effect is very weak for the side region and very strong for the end region. In addition, the optimal orientation/direction axes (indicated by arrows) for the side region is at 74/254 deg, and for the end region is at 50/230 deg, 24 deg towards the left side. It is interesting to note that the maximal inhibition for the entire surround is at 38/218 deg, an axis lying not in between, but 12 deg more towards the left. These differences suggest that the side region and end region may have different underlying cortical circuitry. In Fig. 13(D) a quantitative comparison is shown between the algebraic sum of the side and end inhibition (solid curve) and the actual inhibition of the entire surround (dotted curve). It can be seen that the entire surround inhibition is not simply a linear sum of the effect of the two areas. Similar differences in orientation/direction axes between the two regions and nonlinear summation were also observed for the other two cells.

The selectivity or non-selectivity for movement direction of the IF was also revealed in the orientation/direction tuning curves. The direction selectivity of RF and IF were assessed separately by calculating the same *direction index* (DI) for each:

$$\mathrm{DI} = (P - N)/(P - S)$$

where P and N are the peak (for RF and facilitatory IF) or trough (for inhibitory IF) firing rates to the preferred and non-preferred directions of motion, respectively; S is the spontaneous discharge rate (for RF) or the sustained discharge rate (for IF) measured when RF is stimulated by the central grating alone.

In Fig. 14 the direction selectivity of the IF is compared to the direction selectivity of the RF in two individual cells. The excitatory responses (thin curve) of the cell in Fig. 14(A) are highly direction selective, showing high discharge rates to movement in one direction but none in the opposite direction (DI = 1.0). When the central conditioning grating was drifted in the preferred direction (142 deg), the inhibition tuning curve of the IF had two peaks: one coincided approximately with the cell's optimal direction at 132 deg, the other was 180 deg apart (312 deg). The equal strength of inhibition at the two peaks suggests that the surround inhibition of this cell was non direction-selective (DI = 0), in spite of the fact that the RF of the same cell did show high selectivity for movement direction. Similar results can also be seen in Fig. 11(B) and Fig. 13(A). There were also cells showing better direction selectivity for the IF than for the RF. One example is shown in Fig. 14(B). The RF

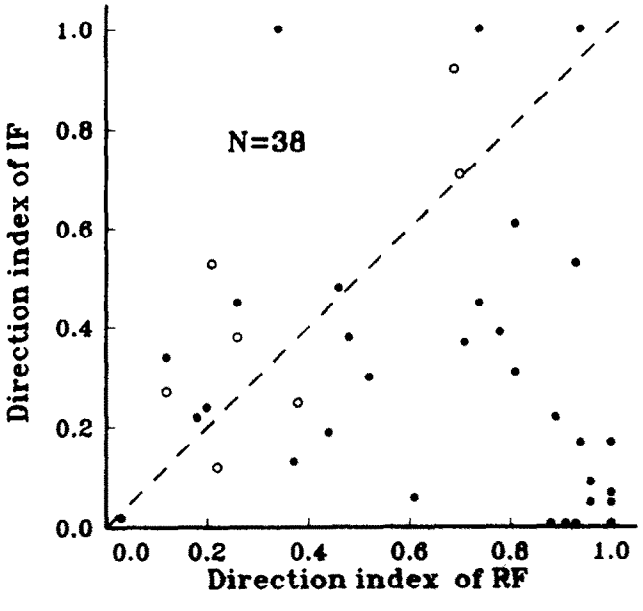

FIGURE 15. Comparison of direction selectivities of RF and IF for 38 striate cells. The direction index of RF is represented on the horizontal axis, whereas direction index of IF is represented on the vertical axis. Open circles denote cells showing facilitatory surround effect, solid circles denote cells showing inhibitory surround effect. The direction index of the four cells showing facilitatory/inhibitory surround effect was > 1.0 and was omitted from this plot. Points below the diagonal line (dashed) indicate that the direction index of IF is lower than that of the RF.

of the cell showed a moderate direction selectivity (DI = 0.38), whereas its IF exhibited a high selectivity.

In Fig. 15 the direction index of IF is plotted against the direction index of RF for 38 cells that showed inhibitory or facilitatory surround effects. The distribution of the points illustrates that, for the majority of the cells, the direction selectivity of IF is lower than that of the RF. This is especially true for cells showing an inhibitory surround effect (solid points), for which 22 out of 31 (71%) are below the diagonal line. The four points lying on the abscissa represent cells for which the RFs were highly direction selective, whereas their IFs were non-direction-selective. There were only about one-quarter of the cells whose IFs showed better direction selectivity than their RFs (the points above the diagonal line).

DISCUSSION

Determination of the IF

It is well known that surrounding the RFs of simple and complex cells in the striate cortex are regions that, although unresponsive to visual stimuli in isolation, have substantial effects on cell responsiveness. The effects of these regions can be either facilitatory or inhibitory (Blakemore & Tobin, 1972; Bishop *et al.*, 1973; Maffei & Fiorentini, 1976; Rizzolatti & Camarda, 1977; Nelson & Frost, 1978, 1985; Hammond & Mackay, 1981; De Valois *et al.*, 1985). The extent of these regions was estimated and their stimulus selectivity was investigated in those studies. The influence of the surround has been more frequently reported to be suppressive. Bishop *et al.* (1973) were able to map out powerful, but non-orientation-selective inhibitory regions that extended 2–6 deg beyond the sides of the RF. Using intracellular recordings, Creutzfeldt *et al.* (1974) mapped an inhibitory area 3–4 deg in dia that overlapped the excitatory centre. They found that the inhibitory influences were directional and to some extent orientation selective. Nelson and Frost (1978) found a peripheral, inhibitory area beyond the conventional receptive field of simple and hypercomplex Type I cells that was orientation selective. Maffei and Fiorentini (1976) found both facilitatory and inhibitory regions in the surrounds of simple and complex cells. They reported that the facilitatory surround regions were orientation selective, but the inhibitory regions were not very selective for orientation. They also found that the facilitatory and inhibitory surround regions were tuned for the spatial frequency of sine-wave gratings. They estimated that these surround regions were three times the size of the RFs. Fries *et al.* (1977) found that simple and complex cells have orientation-selective surrounds that are sometimes directionally selective as well. Using a two-stimulus paradigm, Rizzolatti and Camarda (1977) found very weak effects from areas more than 30 deg beyond the RF. The discrepancies in dimension, tuning properties and polarity of the surround areas seen between different studies are probably due to the choice of different stimulus paradigms, some of them possibly not sufficiently effective to reveal and characterise the "silent" and less sensitive surround influences.

In the present experiments, the RFs were accurately delimited with testing procedures showing better sensitivity than the conventional mapping procedures. This is essential to ensure that peripheral stimulation was presented exclusively outside the RF's extent and to clearly distinguish the excitatory area of the RF from the facilitatory IF [see e.g. Figs 3(A) and 4(A)]. Before we started to determine the extent of the IF and its tuning properties, great care was taken to optimize the stimulus parameters of orientation/direction, spatial frequency and movement speed for the RF. Controlling the concentric, grating patterns by computer enabled both the RF and IF of the cells to be quantitatively studied and the different interactions between the two fields to be examined parametrically. We found three types of surround integration—facilitation, inhibition and disinhibition—beyond both the ends and the sides of the classical receptive fields. These results contradict the observations of Henry, Goodwin and Bishop (1978), who claimed that there is much poorer summation for stimulus width than length. The discrepancy may be due to differences in stimulation techniques. By increasing bar width, luminance is increased, but this does not facilitate the cells responding: as the grating patch becomes wider, the greater number of visible cycles provide more local contrast, thus making the stimulus more effective for cortical cells. The extent of the IFs in our sample (n = 122) varied considerably, and was most frequently 2–5 times the size of the RFs [see Fig. 6(C, D)]. The distribution of dimensions of the IFs' extent is very similar to that reported by De Valois *et al.* (1985), although in their data the extent of the areas was represented by the optimum number of stimulus cycles. Inter-cell differences in the extent of the IFs, the similarity or dissimilarity in integration polarity (inhibition or facilitation) for the width and length axes and the different degrees of surround effects may explain the discrepancies in surround effects described by various authors, and may well illustrate the complexity of spatial integration functions in striate cortex neurons.

It is quite probable that the integration area overlaps the excitatory RF at its centre. Intracellular recordings from the cat striate cortex have shown that stimulation of the excitatory RF elicits both EPSPs and IPSPs (Creutzfeldt *et al.*, 1974; Ferster, 1986) and that the orientation selectivity of IPSPs matches that of EPSPs (Ferster, 1986). The notion is also supported by the extracellular study of DeAngelis, Robson, Ohzawa and Freeman (1992). They presented a sinusoidal grating patch at the optimal orientation and a superimposed grating patch having an orthogonal orientation: both gratings were presented entirely within the excitatory RF. In this case, they demonstrated cross-orientation suppression from within the excitatory RF for most cortical cells. Although they attempted to distinguish this localized inhibition from surround inhibition, their results showed that these do not differ substantially. As

they have described, the suppression within the RF is "somewhat stronger over a range of orientations similar to, but somewhat broader than, the range of excitatory orientations". The weak orientation selectivity of the suppression might be due to the fact that they used local stimulus patterns and that they relied on cross-orientation to avoid excitatory stimulation of the neuron in the spatial domain, and mismatched spatial frequency to avoid excitatory stimulation in the orientation domain. Each would diminish the strength and modulation extent of the suppression.

Cortical and subcortical contributions

It is known that, for retinal ganglion cells and cells of the lateral geniculate body, stimuli presented far beyond the RF may strongly influence neuronal responses to stimuli presented within the RF centre (McIlwain, 1964; Levick, Cleland & Dubin, 1972). By analysing the length- and/or area–response functions of lateral geniculate neurons (Li & He, 1987) and retinal ganglion cells (Li *et al.*, 1991, 1992) in cat, we have demonstrated an extensive, disinhibitory region (DIR) in both X- and Y-cells outside the inhibitory surround of those cells' classical RFs. The spatial summation properties of retinal ganglion cells were found to be very similar to those of the LGN cells, in that they had similar extent and occurred at the same intensity level. More direct evidence indicating a retinal origin of the DIR has been provided from simultaneous recordings of the activities of an LGN neuron and its retinal input (the S-potentials). The close similarities in the length–response functions at these two levels, suggested that the DIR of LGN neurons may simply reflect a property that already exists in the retina. The present study shows that the extent of the IFs of striate cortex neurons, varying between 6 and 18 deg in dia, is within the same range as the DIR of lateral geniculate and retinal ganglion cells, suggesting that the existence of an integration area beyond the conventional RF of cortical neurons can be traced back to their subcortical inputs.

A substantial difference between the cortical and subcortical integration areas is that IF shows a clear orientation selectivity, whereas DIR is non-orientation-selective. The orientation selectivity of the IFs suggests a cortical origin, and the co-orientation property between IF and RF requires wide spatial integration within neighbouring orientation columns. Using multiple electrode cross-correlation techniques, Michalski, Gerstein, Czarkowska and Tarnecki (1983) have provided a direct, functional demonstration of intracortical connections spanning 1 mm and presumed to be intercolumnar; coupled cells were tightly matched in orientation tuning. It is highly probable that after receiving the non-specific subcortical inputs, the striate cells receive further specific modulations in activity through intracortical interconnections.

Intracortical neuronal mechanisms

From studies in which single, striate cortex neurons were injected with horseradish peroxidase, it has been

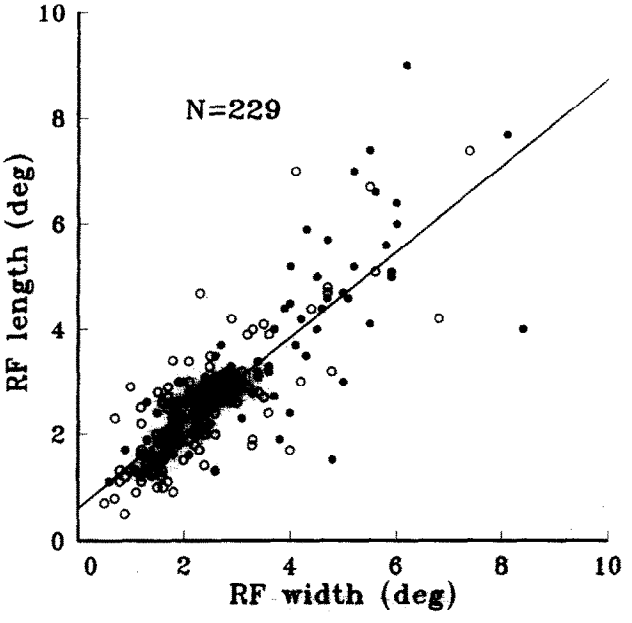

FIGURE 16. Relationship between RF width and RF length for a sample of 229 striate cells. The RF dimensions were determined by grating patch (G-RF). Open circles represent the extent of simple cells and solid circles, complex cells. The oblique line is regression line (slope = 0.81, $r = 0.82$, $P < 0.001$).

reported that the axons of pyramidal cells extend parallel to the brain's surface for distances from 4 mm (Gilbert & Wiesel, 1983) up to 8 mm (Hirsch & Gilbert, 1991), and that collaterals within the axonal fields distribute in repeating clusters with an average periodicity of about 1 mm. The latter are thought to link columns with similar orientation specificity (Ts'o, Gilbert & Wiesel, 1986), thereby allowing cells to integrate visual inputs over an extensive area, although the temporal dispersion of the coupling (broad correlogram peaks) and pharmacological data (their Fig. 10) suggest that long, polysynaptic pathways may participate and the orientation match is only within about 30–40 deg. From the data of Tusa, Palmer and Rosenquist (1978), it can be calculated that a 6 mm axon in area 17 of cat visual cortex would connect points with a retinotopic separation of 6 deg or more at an eccentricity of 5 deg. In the present study, particular care was taken to differentiate the excitatory RF regions from their facilitatory integration area using appropriate tests [see Figs 3(A), 4(A) and 5(A)]. Figure 16 shows the relationship between width and length of the classical RFs in 229 cells (134 simple, 95 complex). The plot shows that the width and length of the receptive fields are significantly correlated ($r = 0.82$, $P < 0.001$). The slope (0.81) of the regression line indicates that, for most cells, the length and width of the RFs were of similar dimension and thus the RFs can be broadly described as a circular area. It can be seen that 64.6% (148 cells) of the total number of cells and 76.1% (102/134) of simple cells (represented by open circles) had RFs of < 3 deg dia (within 10 deg eccentricity), so that these long axons could not deliver visual drive for RF genesis without making the excitatory region of the target neurons' RFs too big. It is more likely that the

long-range, periodically clustered, intrinsic connections participate in elaboration of the stimulus-specific integration field because: (a) the IF covers an extensive range: for more than 70% of the cells examined, both the width and length of the IFs were larger than 6 deg; (b) the IF exhibits similar orientation and spatial frequency selectivity as the RF for each individual cell.

IFs differ from RFs in that they cannot drive the cell directly, but can only facilitate or inhibit the cell response to stimuli located inside the RF. The synaptic mechanisms that may underlie this property were examined in slices of cat's striate cortex using electrical pulses applied at a lateral distance of 0.9–3 mm in layers 2 + 3 (Hirsch & Gilbert, 1991). It was found that activating remote lateral fibres can inhibit as well as excite their postsynaptic targets. At the resting membrane potential, however, the laterally evoked EPSP was too small to trigger action potentials. This observation illustrates that the role of the intracortical horizontal connections is to modulate rather than generate activity within the target columns. In *in vivo* intracellular studies of cat striate cortex, IPSPs were evoked by distant visual stimuli. This remote inhibitory effect was thought to be mediated monosynaptically by basket cells, which have axons extending for a millimeter or more (Martin, Somogyi & Whitteridge, 1983; Somogyi, Kisvárday, Martin & Whitteridge, 1983).

Possible functional significance

For most cells, the tuning properties of the IFs in the domains of orientation, spatial frequency and movement speed were all found to be similar to those of the RFs. The close similarities in most filtering properties between these two fields indicate that an individual cell integrates information from a large part of the visual field, and that visual information can be integrated (positively or negatively) over a wide space only for those components that share similar orientation, spatial frequency and movement speed, and therefore are highly correlated in time and space. These specific interactions seem ideally suited for Julesz's theory concerning the mechanisms of texture perception. In his recent model (Julesz, 1981a, b; Julesz & Bergen, 1983), Julesz proposed that texture discrimination is based on the detection of distinct structure elements ("textons"), which are based on differences in orientation, spatial frequency, motion, etc. in various regions of a pattern. Nothdurft and Li (1984, 1985) have investigated the responses of single cells in the cat striate cortex to different texture patterns consisting of arrays of lines. The line elements within a central disk were oriented orthogonally to the line elements outside. They projected the stimulus patterns onto a tangent screen with the central texture field matching the cell's optimal orientation. The pattern was systematically moved under computer control, so that each part of the pattern traversed the cell's RF (with its surround area). Spikes were accumulated into a 50 × 50 bin raster, each bin representing the neuron's response when a particular part of the stimulus pattern moved across the RF centre. The number of spikes in each bin was then plotted in a two dimensional display as different densities and the "response pattern" of the cells was derived. Successful texture discrimination by the cell was indicated by a disk-shaped area at the centre of the response patterns [see Figs 3(a) and 4(a) (Nothdurft & Li, 1985)]. Both simple and complex cells were able to distinguish texture areas based on the orientation differences of the elementary lines, even when the individual lines were not resolved in their responses. For some cells, border enhancement was seen between areas of different texture orientation [see Figs 4(a) and 8(f) (Nothdurft & Li, 1985)]. The border enhancement based on orientational differences could be explained by the findings of this report that the inhibitory IFs often exert facilitatory effects on the cell response when the surround grating was oriented at non-optimal orientations [see Figs 11(B) and 13], and similarly, facilitatory IFs also exert inhibition when surround gratings were oriented non-optimally. This is a representation of Mach-type contrast in the domain of orientation sensitivity.

We have not attempted to put forward a model of orientation selectivity based on the present study. However, the existence of the parametrically tuned surround suggests to us that a satisfactory model should take into consideration the effects from the extensive surround. Henry, Dreher and Bishop (1974) attributed orientation selectivity and Bishop, Henry and Smith (1971) attributed disparity tuning to the inhibitory sidebands of simple cells. Our results show that the tuning properties of striate cells are generated within the classical RF, and regions beyond the RF may play a role in sharpening the feature selectivities and enhancing the feature contrasts between neighbouring fields. In the present study, tuning properties of the RFs were measured by the use of a local grating patch covering exclusively the excitatory area, while the surround areas (both the side and end regions) were uniformly illuminated. The tuning curves thus obtained reflect feature selectivities of the RFs without the assistance of the side and end areas. In this situation, the cells still showed substantially normal tuning properties in orientation/direction, spatial frequency and speed of movement (see the thin curves in Figs 7, 9, 11 and 14, respectively). On the other hand, when comparing the tuning functions of the IF to that of the RF, in these domains, for individual cells, IF tuning bandwidth was broader than the RF tuning widths [see Figs 8(B), 10(B) and 12(B)]. As expected, when the RF and the IF were stimulated simultaneously with an extended grating, orientation tuning width of the cells became narrower, and selectivity was sharper [see Fig. 12(C)]. By using different lengths of a moving bar stimulus, similar observations were reported for the (inhibitory) end-zone of simple, complex and hypercomplex I cells (Henry, Bishop & Dreher, 1974; Henry *et al.*, 1974; Orban *et al.*, 1979) and for simple cells having facilitatory flanks at the end regions (Rose, 1977). The orientation tuning curve progressively sharpened as the stimulus bar was lengthened.

The specific interactions between IF and RF may correlate with the psychophysical phenomenon that

perception of a feature in one part of the visual field is influenced by the visual context in which that feature is presented. Nelson (1985) and Gilbert and Wiesel (1990) have accounted for orientation contrast illusions on the basis of orientation domain interactions between a neuron's classic RF and the area beyond it. The contrast enhancement of orientation between neighbouring texture areas could also be explained on the basis of the orientation interactions between IF and RF. As is seen in the inhibitory interactions [Fig. 11(A, B)], the response of the cells reaches a minimum when surround and centre gratings are at the same orientation, the response increases toward the control level when the surround is oriented away from the centre orientation.

Contrast illusions of speed of motion have been documented in psychophysical experiments by many authors (Walker & Powell, 1974; Tynan & Sekuler, 1975; Marshak & Sekuler, 1979; Mather & Moulden, 1980), but little is known about the cellular mechanisms causing these phenomena. Tynan and Sekuler (1975) used a centre and surround of spatially random dots to study the effect of surround motion on the centre. The perceived centre speed reaches a minimum when surround and centre are moving at the same speed (in the same direction). The functions that relate perceived speed of the centre to surround speed are in good agreement with the speed selective effects of IF on RF. As can be seen in Figs 9 and 10(A), the cells were inhibited maximally when centre and surround moved at the same speed, and the response increased when surround speed was different from the optimal speed of the centre.

REFERENCES

Bishop, P. O., Coombs, J. S. & Henry, G. H. (1973). Receptive fields of simple cells in the cat striate cortex. *Journal of Physiology, London, 231*, 31–60.

Bishop, P. O., Henry, G. H. & Smith, C. J. (1971). Binocular interaction fields of single units in the cat striate cortex. *Journal of Physiology, London, 216*, 39–68.

Bishop, P O., Kozak, W. S., Levick, W. R. & Vakkur, G. J. (1962). The determination of the projection of the visual field on the lateral geniculate nucleus in the cat. *Journal of Physiology, London, 163*, 503–539.

Blakemore, C. & Tobin, E. A. (1972). Lateral inhibition between orientation detectors in the cat's visual cortex. *Experimental Brain Research, 15*, 439–440.

Cleland, B. G., Dubin, M. W. & Levick, W. R. (1971). Sustained and transient neurons in the cat's retina and lateral geniculate nucleus. *Journal of Physiology, London, 217*, 473–496.

Creutzfeldt, O. D., Kuhnt, U. & Beneveto, L. A. (1974). An intracellular analysis of visual cortical neurones to moving stimuli: Responses in a cooperative neuronal network. *Experimental Brain Research, 21*, 251–274.

DeAngelis, G. C., Robson, J. G., Ohzawa, I. & Freeman, R. D. (1992). Organization of suppression in receptive fields of neurons in cat visual cortex. *Journal of Neurophysiology, 68*, 144–163.

De Valois, R. L., Thorell, L. G. & Albrecht, D. G. (1985). Periodicity of striate-cortex-cell receptive fields. *Journal of the Optical Society of America A, 2*, 1115–1122.

Fernald, R. & Chase, E. (1971). An improved method for plotting retinal landmarks and focusing the eyes. *Vision Research, 11*, 95–96.

Ferster, D. (1986). Orientation selectivity of synaptic potentials in neurons of cat primary visual cortex. *Journal of Neuroscience 6*, 1284–1301.

Fischer, B. & Krüger, J. (1974). The shift effect in the cat's lateral geniculate neurons. *Experimental Brain Research, 21*, 225–227.

Fries, W., Albus, K. & Creutzfeldt, O. D. (1977). Effects of interacting visual patterns on single cell responses in cat's striate cortex. *Vision Research, 17*, 1001–1008.

Gilbert, C. D. & Wiesel, T. N. (1983). Clustered intrinsic connections in cat visual cortex. *Journal of Neuroscience, 3*, 1116–1133.

Gilbert, C. D. & Wiesel, T. N. (1990). The influence of contextual stimuli on the orientation selectivity of cells in primary visual cortex of the cat. *Vision Research, 30*, 1689–1701.

Hammond, P. & MacKay, D. M. (1981). Modulatory influences of moving textured backgrounds on responsiveness of simple cells in feline striate cortex. *Journal of Physiology, London, 319*, 431–442.

Henry, G. H., Bishop, P. O. & Coombs, J. S. (1969). Inhibitory and sub-liminal excitatory receptive fields of simple units in cat striate cortex. *Vision Research, 9*, 1289–1296.

Henry, G. H., Bishop, B. O. & Dreher, B. (1974). Orientation, axis and direction as stimulus parameters for striate cells. *Vision Research, 14*, 767–777.

Henry, G. H., Dreher, B. & Bishop, B. O. (1974). Orientation specificity of cells in cat striate cortex. *Journal of Neurophysiology, 37*, 1394–1409.

Henry, G. H., Goodwin, A. W. & Bishop, P. O. (1978). Spatial summation of responses in receptive fields of single cells in cat striate cortex. *Experimental Brain Research, 32*, 245–266.

Hess, R., Negishi, K. & Creutzfeldt, O. D. (1975). The horizontal spread of intracortical inhibition in the visual cortex. *Experimental Brain Research, 22*, 415–419.

Hirsch, J. A. & Gilbert, C. D. (1991). Synaptic physiology of horizontal connections in the cat's visual cortex. *Journal of Neuroscience, 11*, 1800–1809.

Hubel, D. H. & Wiesel, T. N. (1962). Receptive fields, binocular interaction and functional architecture in the cat's visual cortex. *Journal of Physiology, London, 160*, 106–154.

Hubel, D. H. & Wiesel, T. N. (1965). Receptive fields and functional architecture in two nonstriate visual areas (18 and 19) of the cat. *Journal of Neurophysiology, 28*, 229–289.

Ikeda, H. & Wright, M. J. (1972a). Receptive field organization of "sustained" and "transient" retinal ganglion cells which subserve different functional roles. *Journal of Physiology, London, 227*, 769–800.

Ikeda, H. & Wright, M. J. (1972b). Functional organization of the periphery effect in retinal ganglion cells. *Vision Research, 12*, 1857–1879.

Ikeda, H. & Wright, M. J. (1972c). The outer disinhibitory surround of the retinal ganglion cell receptive field. *Journal of Physiology, London, 226*, 511–544.

Jones, B. H. (1970). Response of single neurons in cat visual cortex to a simple and more complex stimulus. *American Journal of Physiology, 218*, 1102–1107.

Julesz, B. (1981a). Textons, the elements of texture perception, and their interactions. *Nature, London, 290*, 91–97.

Julesz, B. (1981b). A theory of preattentive texture discrimination based on first-order statistics of textons. *Biological Cybernetics, 41*, 131–138.

Julesz, B. & Bergen, J. R. (1983). Textons, the fundamental elements in preattentive vision and perception of textures. *Bell System Technical Journal, 62*, 1619–1645.

Krüger, J. (1977). Stimulus dependent color specificity of monkey lateral geniculate neurones. *Experimental Brain Research, 30*, 297–311.

Krüger, J. & Fischer, B. (1973). Strong periphery effect in cat retinal ganglion cells. Excitatory responses in ON- and OFF-center neurons to single grid displacement. *Experimental Brain Research, 18*, 316–318.

Levick, W. R., Cleland, B. G. & Dubin, M. W. (1972). Lateral geniculate neurons of cat: Retinal inputs and physiology. *Investigative Ophthalmology and Visual Science, 11*, 302–311.

Li, C. Y. & He, Z. J. (1987). Effects of patterned backgrounds on responses of lateral geniculate neurons in cat. *Experimental Brain Research, 67*, 16–26.

Li, C. Y., Pei, X., Zhow, Y. X. & Mitzlaff, H. C. (1991). Role of the

extensive area outside the X-cell receptive field in brightness information transmission. *Vision Research, 31*, 1529–1540.

Li, C. Y., Zhou, Y. X., Pei, X., Qiu, F. T., Tang, C. Q. & Xu, X. Z. (1992). Extensive disinhibitory region beyond the classical receptive field of cat retinal ganglion cells. *Vision Research, 32*, 219–228.

Maffei, L. & Fiorentini, A. (1976). The unresponsive regions of visual cortical receptive fields. *Vision Research, 16*, 1131–1139.

Marlin, S. G., Hasan, S. J. & Cynader, M. S. (1988). Direction-selective adaptation in simple and complex cells in cat striate cortex. *Journal of Neurophysiology, 59*, 1314–1330.

Marrocco, R. T., McClurkin, J. W. & Young, R. A. (1982). Modulation of lateral geniculate nucleus cell responsiveness by visual activation of the cortico-geniculate pathway. *Journal of Neuroscience, 2*, 256–263.

Marshak, W. & Sekuler, R. (1979). Mutual repulsion between moving visual targets. *Science, 205*, 1399–1401.

Martin, K. A. S., Somogyi, P. & Whitteridge, D. (1983). Physiological and morphological properties of identified basket cells in cat's visual cortex. *Experimental Brain Research, 50*, 193–200.

Mather, G. & Moulden, B. (1980). A simultaneous shift in apparent direction: Further evidence for a "distribution-shift" model of direction coding. *Quarterly Journal of Experimental Psychology, London, 32*, 325–333.

McIlwain, J. T. (1964). Receptive fields of optic tract axons and lateral geniculate cells: Peripheral extent and barbiturate sensitivity. *Journal of Neurophysiology, 27*, 1154–1173.

McIlwain, J. T. (1966). Some evidence concerning the physiological basis of the periphery effect in the cat's retina. *Experimental Brain Research, 1*, 265–271.

Michalski, A., Gerstein, G. L., Czarkowska, J. & Tarnecki, R. (1983). Interactions between cat striate cortex neurons. *Experimental Brain Research, 51*, 97–107.

Movshon, J. A. & Lennie, P. (1979). Pattern-selective adaptation in visual cortical neurons. *Nature, London, 278*, 850–852.

Nelson, J. I. (1985). The cellular basis of perception. In Rose, D. & Dobson, V. G. (Eds), *Models of the visual cortex* (pp. 108–122). Chichester: Wiley.

Nelson, J. I. & Frost, B. J. (1978). Orientation selective inhibition from beyond the classic visual receptive field. *Brain Research, 139*, 359–365.

Nelson, J. I. & Frost, B. J. (1985). Intracortical facilitation among co-oriented co-axially aligned simple cells in cat striate cortex. *Experimental Brain Research, 61*, 54–61.

Nothdurft, H. C. & Li, C. Y. (1984). Representation of spatial details in textured patterns by cells of the cat striate cortex. *Experimental Brain Research, 57*, 9–21.

Nothdurft, H. C. & Li, C. Y. (1985). Texture discrimination: Representation of orientation and luminance differences in cells of the cat striate cortex. *Vision Research, 25*, 99–113.

Orban, G. A., Kato, H. & Bishop, P. O. (1979). End-zone region in receptive fields of hypercomplex and other striate neurons in the cat. *Journal of Neurophysiology, 42*, 818–832.

Rizzolatti, G. & Camarda, R. (1977). Influence of the presentation of remote visual stimuli on visual responses of cat area 17 and lateral suprasylvian area. *Experimental Brain Research, 29*, 107–122.

Rose, D. (1977). Responses of single units in cat visual cortex to moving bars of light as a function of bar length. *Journal of Physiology, London, 271*, 1–23.

Skottun, B. C., De Valois, R. L., Grosof, D. H., Movshon, A., Albrecht, D. G. & Bond, A. B. (1991). Classifying simple and complex cells on the basis of response modulation. *Vision Research, 31*, 1079–1086.

Somogyi, P., Kisvárday, Z. F., Martin, K. A. C. & Whitteridge, D. (1983). Synaptic connections of morphologically identified and physiologically characterized large basket cells in the striate cortex of cat. *Neuroscience, 10*, 261–294.

Ts'o, D., Gilbert, C. D. & Wiesel, T. N. (1986). Relationships between horizontal connections and functional architecture in cat striate cortex as revealed by cross-correlation analysis. *Journal of Neuroscience, 6*, 1160–1170.

Tusa, R. J., Palmer, L. A. & Rosenquist, A. C. (1978). The retinotopic organization of Area 17 (striate cortex) in the cat. *Journal of Comparative Neurology, 177*, 213–236.

Tynan, P. & Sekuler, R. (1975). Simultaneous motion contrast: Velocity, sensitivity and depth response. *Vision Research, 15*, 1231–1238.

Walker, P. & Powell, D. J. (1974). Lateral interaction between neural channels sensitive to velocity in human visual system. *Nature, London, 252*, 732–733.

Acknowledgements—This research was supported by the National Natural Science Foundation of China (No. 39330110), the National Science Council of China (BFCM-LI) and partly by the Laboratory of Visual Information Processing of the Chinese Academy of Sciences. We thank Dr D. A. Tigwell and Mrs J. Dames for English correction and Mrs X. C. Hsu for technical assistance.